# Targetable *BIRC5* dependency in therapy-resistant *TP53* mutated acute myeloid leukemia

**Authors:** Ahmed M. Mamdouh[1*], Fang Qi Lim[1*], Yang Mi[1], Elyse A. Olesinski[2], Cheryl Gek Teng Chan[1], Shaista Jasdanwala[1], Xiao Xian Lin[1], Yichen Wang[1], Jordan Yong Ming Tan[1], Karanpreet Singh Bhatia[1], Valeriia Sapozhnikova[3,4,5], Chuqi Wang[1], Aarthi Nivasini Mahesh[1], Daniel Tan En Liang[1], Nishtha Chitkara[1], Philipp Mertins[5,6], Leah Hogdal[7], Brandon D. Brown[8], Torsten Haferlach[9], Camille Lobry[10], Coleman Lindsley[7], Alexandre Puissant[10], Han Kiat Ho[1], Sanjukta Das[11], Anthony Letai[7], Steven M. Kornblau[8], Jan Krönke[3,4], Edward Ayoub[12], Koji Itahana[13], Michael Andreeff[8], Shruti Bhatt[1,14]

**Affiliations**

[1]Department of Pharmacy, National University of Singapore, Singapore.
[2]Boston University Chobanian & Avedisian School of Medicine, Boston, MA, USA.
[3]Department of Hematology, Oncology and Cancer Immunology, Charité - Universitätsmedizin Berlin, corporate member of Freie Universität Berlin and Humboldt-Universität zu Berlin, Berlin, Germany.
[4]German Cancer Consortium (DKTK) partner site Berlin and German Cancer Research Center (DKFZ), Heidelberg, Germany.
[5]Max Delbrück Center for Molecular Medicine, Berlin, Germany.
[6]Berlin Institute of Health (BIH), Berlin, Germany.
[7]Dana-Farber Cancer Institute, 440 Brookline Avenue, M430, Boston, MA, USA.
[8]Division of Pediatrics, The University of Texas M.D. Anderson Cancer Center, Houston, TX, USA.
[9]MLL Munich Leukemia Laboratory, Munich, Germany.
[10]Université de Paris, Génomes, Biologie Cellulaire et Thérapeutique U944, INSERM, CNRS, Paris, France.
[11]School of Biotechnology, KIIT University, Odisha, India.
[12]Department of Leukemia, The University of Texas M.D. Anderson Cancer Center, Houston, TX, USA.
[13]Programme in Cancer & Stem Cell Biology, Duke-NUS Medical School, Singapore.
[14]Department of Hematology & Medical Oncology, Emory School of Medicine

*Authors contributed equally.

**Running Title:** *TP53* governs post-mitochondrial death

**Keywords:** AML, *TP53* mutation, mitochondrial priming, inhibitors of apoptosis, Survivin

**Corresponding Authors**

1. Shruti Bhatt, PhD

National University of Singapore

Department of Pharmacy

Science Drive 3, Blk S7, 02-16

Singapore, 129788

Email: shruti_bhatt@nus.edu.sg

Phone: +65-65168014

Department of Hematology and Medical Oncology

Emory School of Medicine and the Winship Cancer Institute

Emory University, Atlanta, GA, 30322, USA

Email: shrutiben.bhatt@emory.edu

**Acknowledgments**

S.B. acknowledges support from the Singapore Ministry of Education (MOE) Academic Research Fund (AcRF) Tier 2 (MOE-000573-00), NUS-Paris University Joint Grant, the Department of Pharmacy and Pharmaceutical Sciences Starup Funds at National University of Singapore. S.B. is a recipient of the EMBO Global Investigator Award. A.M.M. acknowledges support from the Singapore International Graduate Award (SINGA). A.L. acknowledges support from P01 CA066996 and Ludwig Center at Harvard. A.P. acknowledges support by ERC CoG (DynAML, 101088563) and LNCC (EL2024-PUISSANT) grants. J.K. acknowledges support from the José Carreras Leukämie-Stiftung (project DJCLS 07 R/2024), the Deutsche Forschungsgesellschaft (DFG KR 3886/8-1), and the Deutsche Konsortium für Translationale Krebsforschung (DKTK). R.C.L. was supported

by a Scholar award from The Leukemia & Lymphoma Society (RCL) and the Edward P. Evans Center for Myelodysplastic Syndrome at Dana-Farber Cancer Institute.

**Disclosures and Conflicts of Interest**

A.L. owns stocks in Zentalis, Flash Therapeutics, Dialectic, and provided consultancy for Zentalis, Flash Therapeutics, Anji Onco, and Dialectic Therapeutics. M.A. provided consultancy for Aptose, Eterna, GlycoMimetics, and SentiBio. J.K. provided consultancy for Janssen, Takeda, Abbvie, Jazz Pharmaceuticals, Sanofi, Astra Zeneca, and Pfizer. R.C.L. provided consultancy for Takeda Pharmaceuticals, Bluebird bio, Qiagen, Sarepta Therapeutics, Verve Therapeutics, Jazz Pharmaceuticals, and Vertex Pharmaceuticals. T.H. has equity ownership of MLL Munich Leukemia Laboratory. L.H. owns stocks in and provided consultancy for Pfizer.

**Data Availability Statement**

Cell line RNA-seq data has been deposited in the Gene Expression Omnibus database under accession numbers. Cell line proteomics data and whole-genome CRISPR screen data will be available on request. Primary sample bulk RNA-seq data generated in this study are not publicly available due to patient privacy requirements and were used under license for this study. Primary sample proteomics data and single-cell data will be available from the authors upon request.

**ABSTRACT**

*TP53* mutations confer treatment resistance across multiple cancers. Mechanisms of therapy resistance, beyond affecting transactivation of BCL-2 family genes, remain a mystery. Here, we report that *TP53* mutated AML, triple negative breast cancer, and colorectal cancer escape therapy-induced apoptosis due to inability to activate caspase-3/7, despite having normal mitochondrial outer membrane permeabilization (MOMP) induction. To identify post-MOMP determinants of therapy resistance in *TP53* mutated AML, we applied a multiomics approach – whole-genome CRISPR screen, bulk/single-cell RNAseq, and high-throughput drug screen. *BIRC5*, encoding survivin, was selectively upregulated in paired hematopoietic stem/multipotent progenitor cells from *TP53* mutant AML patients, with further enrichment after venetoclax-azacitidine (VenAza) relapse. Critically, *BIRC5* was also upregulated in 17 of 26 *TP53* mutant TCGA cancers. Genetic ablation of *BIRC5* resensitized *TP53* mutated AML to standard therapy by restoring caspase activation, validating therapeutic relevance. Importantly, targeting IAPs and survivin using clinically relevant inhibitors overcame VenAza resistance of *TP53* mutant tumors *in vivo*, achieving sustained AML suppression. Combination with survivin inhibitors also overcame chemotherapy resistance in *TP53* deficient solid cancers. Together, we discovered that wild-type *TP53* is required in post-MOMP signaling and that *BIRC5* dependency is an effective therapeutic target for poor prognosis, *TP53* mutated cancers.

## INTRODUCTION

*TP53* mutations or deletions are drivers for therapy resistance in most cancers due to poor patient responses to chemotherapy and targeted therapy.[1–3] Among cancers with *TP53* mutations, acute myeloid leukemia (AML), an aggressive form of blood cancer, has particularly dire outcomes. *TP53* mutations are found in 10% of *de novo* AML, 20-35% of therapy-related myeloid neoplasia, and 70-80% of complex karyotype AML (CK-AML).[4 5,6] The introduction of venetoclax (BCL-2 inhibitor) combined with azacitidine (hypomethylating agent) (VenAza) has transformed outcomes for many AML patients,[7] particularly with poor-risk cytogenetics and wild-type *TP53* who historically responded poorly to 7+3.[8–11 7]However, the effectiveness of this therapeutic advance is diminished in patients harboring *TP53* mutations, where co-presence of poor-risk cytogenetics and *TP53* mutations drastically reduces overall survival from 23.4 months to 5.2 months.[7] Therefore, *TP53* mutations appear as a major driver of VenAza resistance even without poor-risk cytogenetics. This profound effect is reflected in the broader AML population, where *TP53* mutant AML patients have shorter relapse-free survival (4.3 months vs 18.9 months) and overall survival (5.2 months vs 19.4 months) compared to those with wild-type *TP53* AML.[11–13] These consistently poor outcomes across treatment modalities underscore the pressing unmet need to identify treatment strategies that overcome therapy resistance in *TP53* mutated AML.

As a transcription factor, p53 acts as the “guardian of the genome” by binding to specific DNA sequences and transactivating numerous genes to perform canonical functions in response to stress, including maintenance of genomic integrity, cell cycle arrest, and apoptosis induction, as well as non-canonical functions.[11,14] To induce apoptosis, p53 triggers mitochondrial outer membrane permeabilization (MOMP) through transcription or induction of pro-apoptotic proteins, BAX, PUMA, and NOXA,[15,16] or repression of anti-apoptotic

proteins, MCL-1, BCL-2, and BCL-xL.[17,18] Alternatively, cytoplasmic p53 can sequester anti-apoptotic proteins via transcription-independent mechanisms, with disruption of these complexes by PUMA to release p53 to trigger MOMP and apoptosis.[19–21] Although MOMP is traditionally considered the 'point-of-no-return' in apoptotic signaling across diverse cell types responding to therapeutic stress, a study has suggested that MOMP may not be the point of no return and that cells expressing the wild-type p53 may recover following MOMP activation.[22] Aside from the induction of BCL-2 family proteins, these observations imply that there must exist unexplored functions of p53 that become dysregulated to evade apoptosis and mediate therapy resistance. Despite decades of research establishing *TP53* as the master regulator of apoptosis, the mechanisms by which *TP53* mutations confer treatment resistance beyond dysregulation of BCL-2 family proteins have remained enigmatic.

Through systematic analysis, we discovered that *TP53* mutated cells possess specific defects in post-MOMP signaling, enabling their survival even after MOMP activation. This observation prompted us to investigate the molecular mechanisms underlying this phenotype through an unbiased, multiomics approach. Integration of genome-wide CRISPR screening, bulk and single-cell transcriptomics, proteomics, and high-throughput drug screening identified upregulation of the inhibitor of apoptosis protein *BIRC5* (survivin) as a key mediator of this post-MOMP survival. Importantly, this dependency creates a therapeutically exploitable vulnerability across *TP53* mutated cancers, offering a novel strategy to overcome chemoresistance in these aggressive malignancies.

## RESULTS

### *TP53* mutations mediate therapy resistance by evasion of apoptosis

To study mechanisms of resistance and poor treatment outcomes in *TP53* mutated tumors, we engineered *TP53* deficient AML cells using CRISPR/Cas9 genome editing in MOLM-13 and MV-4-11 with two different sgRNAs (Figure 1A and S1A; validation in Figure S1B). *TP53* deletion (knockout) reduced sensitivity towards venetoclax plus azacitidine (VenAza) compared to wild-type *TP53* (Figure 1B). Beyond VenAza in AML, we validated resistance to cytotoxic chemotherapy in two *TP53* deficient cancers: colorectal cancer (CRC) (HCT-116) treated with 5-flurouracil (5-FU) and triple-negative breast cancer (TNBC) (CAL-51) treated with doxorubicin (Dox) (Figure 1B). Besides deletions, *TP53* dysfunction is also caused by inactivating missense mutations.[23] Thus, we exposed a panel of isogenic MOLM-13 cells carrying 6 different missense mutations ($TP53^{-/mut}$ (R175H, R273H, R248Q, R282W, Y220C, M237I)) in the DNA binding domain (DBD), knockout ($TP53^{-/-}$), or matched wild-type ($TP53^{+/+}$) *TP53* to venetoclax, azacitidine, or VenAza (Figure S1C). $TP53^{-/mut}$ cells had varied sensitivities, with $TP53^{-/R248Q}$ cells least sensitive to VenAza (IC50 Ven = 72.5 nM). $TP53^{-/R248Q}$ cells also had higher colony forming units (CFUs) under VenAza treatment compared to $TP53^{+/+}$ (76.9% vs 56.4%; Figure 1C). All six $TP53^{-/mut}$ cell lines had a competitive advantage over $TP53^{+/+}$ cells treated with VenAza (Figure 1D and S1D).

Since *TP53* is activated in response to stress, we hypothesized that dysfunction in canonical functions (cell cycle, apoptosis, senescence, DNA damage) may drive reduced cytotoxicity in $TP53^{-/mut}$ cells. Cell cycle profiles showed less accumulation of $TP53^{-/mut}$ cells in sub-G1 phase after VenAza treatment, yet G1 arrest or senescence was not observed in all genotypes (Figure S2A-C). Apoptosis was severely inhibited in all $TP53^{-/mut}$ and $TP53^{-/-}$ cells under VenAza and standard chemotherapy, cytarabine, and etoposide (Figure 1E). Apart from

MOLM-13, additional validation in MV-4-11, CAL-51, and HCT-116 cells with *TP53*$^{-/-}$ showed reduced apoptosis in response to standard of care therapy (Figure 1F). This suggests apoptosis evasion as a conserved mode of resistance to multiple treatment types across *TP53* deficient cancers. To next test whether reduced apoptosis in *TP53* mutated cells was attributed to DNA damage, we performed alkaline comet assays. DNA damage was increased after VenAza treatment compared to DMSO in *TP53*$^{+/+}$ cells (Figure 1G). However, *TP53*$^{-/mut}$ cells exhibited greater DNA damage at baseline, which remained largely unchanged after VenAza treatment (Figure 1G and S2D-E). Overall, our findings show that *TP53* mutations drive resistance to cytotoxic chemotherapy and targeted agents in AML through defects in apoptosis or DNA damage, rather than sub-G1 phase accumulation and senescence.

**_TP53_ mutated AML has altered BCL-2 family protein expression**

Therapy-induced apoptosis is predominantly regulated by the intrinsic apoptosis pathway via interactions between BCL-2 family proteins in the outer mitochondrial membrane. We next investigated how *TP53* mutant tumors evade apoptosis by interrogating molecular mechanisms of resistance in pre-MOMP, MOMP, and post-MOMP settings. We focused on *R248Q* mutation, since it is the second most common *TP53* mutation in AML[23–25] and conferred higher resistance against VenAza (Figure S1C). Gene set enrichment analysis from RNA-seq demonstrated significant enrichment in p53 signaling with VenAza treatment in only *TP53*$^{+/+}$ cells (NES 1.58, $p < 0.05$), consistent with a recent independent study[25] (Figure S3A). As expected, *TP53* target genes *CDKN1A* and *MDM2* were downregulated in *TP53*$^{-/R248Q}$ and *TP53*$^{-/-}$ cells at baseline (Figure S3B). Since *TP53* regulates apoptotic genes, we hypothesized that VenAza would alter expression of BCL-2 family genes and proteins in a *TP53*-dependent manner. At the mRNA level, pro-apoptotic genes *BAX*, *BBC3* (encodes PUMA), and *PMAIP1* (encodes NOXA) were downregulated in *TP53*$^{-/R248Q}$ cells compared to

compared to *TP53*$^{+/+}$ cells at the baseline as well as in the presence of VenAza (Figure S3B). At the protein level, pro-apoptotic protein BAX was decreased, and the anti-apoptotic protein MCL-1 was increased (Figure 2A and S3C). Conversely, pro-apoptotic proteins BIM-EL, BAK, and BID were upregulated (Figure 2A and S3C). Since BIM can directly interact with and activate BAX and BAK (required for pore formation and MOMP), we further investigated BIM expression levels across multiple tumors. MV-4-11 cells showed upregulation in BIM-EL after *TP53* deletion (Figure S3D). Similarly, primary tumors from the TCGA PanCancer Atlas showed upregulation in BIM for 5/27 tumors at the mRNA level and 10/26 at the protein level (Figure S3E). This emphasizes that despite loss of key pro-apoptotic regulators in *TP53* mutations, the upregulation of BIM and BID may compensate for this downregulation.

BIM sequestration by anti-apoptotic partners can also prevent induction of apoptosis. We and others have previously shown that MCL-1 sequesters BIM from BCL-2 in venetoclax-resistant AML cells,[26–28] which prompted us to evaluate MCL-1 dependence in *TP53*$^{-/R248Q}$ and *TP53*$^{-/-}$ cells. Coimmunoprecipitation of BIM showed reduced BCL-2–BIM interactions while MCL-1–BIM interactions were elevated (Figure 2B). Addition of an MCL-1 inhibitor (S63845) to VenAza sensitized *TP53* mutated cells to apoptosis, supporting our previous studies[29,30] (Figure S3F-G). Although using MCL-1 inhibition to overcome resistance in *TP53* mutated settings is an attractive option, observed cardiotoxicity in recent clinical trials has limited investigation of these agents.[31] Collectively, we found that *TP53* mutations altered the expression of BCL-2 family proteins and their protein-protein interactions.

**MOMP occurs in *TP53* mutated AML despite alternations in BCL-2 family proteins**

Engagement of apoptosis involves MOMP and is often seen as a point of no return. Thus, we wondered if *TP53* mutated cells evade apoptosis by resisting MOMP induction. We performed BH3 profiling assays in unperturbed, permeabilized *TP53*$^{-/mut}$ cells using BH3 peptides derived from pro-apoptotic proteins. Rigorous testing in *TP53*$^{+/+}$ cells, *TP53*$^{-/mut}$ cells, *TP53*$^{-/-}$ cells, two AML cell lines (MOLM-13, MV-4-11) with different *TP53* sgRNAs, and two additional cancers (HCT-116, CAL-51) showed no unique trend and overall, retained capacity for MOMP in response to BIM peptide, implying preservation of apoptotic threshold and ability to undergo MOMP in response to direct stress on the mitochondria (Figure 2C). In *TP53*$^{-/mut}$ cells, dependence on individual anti-apoptotic proteins (BCL-2, (BAD BH3 peptide), MCL-1 (MS-1 BH3 peptide), or BCL-xL (HRK BH3 peptide)) was largely comparable to *TP53*$^{+/+}$ cells (Figure S4A). Further analysis in AML primary tumors revealed similar apoptotic priming to BIM for *TP53*$^{-/mut}$ and *TP53*$^{+/+}$ cells and mitochondrial sensitivity to navitoclax and venetoclax, independent of *TP53* status (Figure 2D and S4B). Additionally, BCL-xL (HRK BH3 peptide) and MCL-1 (NOXA BH3 peptide) dependence were increased (Figure S4B). We eliminated the possibility that conservation of MOMP in *TP53* mutated cells was driven by baseline differences in cytoplasmic cytochrome c levels (Figure S4C). To determine whether *TP53* mutated cells resist MOMP after drug treatment, we performed dynamic BH3 profiling, which showed no loss in MOMP in *TP53*$^{-/mut}$ cells after VenAza as compared to *TP53*$^{+/+}$ cells (Figure 2E). Overall, these findings emphasize that despite *TP53* mutations, functional capacity to engage MOMP remains preserved in AML, indicating that post-MOMP regulation may drive differences in apoptotic outcomes.

**Impaired caspase activation inhibits drug-induced apoptosis in *TP53* mutated cells**

We wondered whether *TP53* mutations cause differences in post-MOMP signaling to drive evasion of apoptosis. Chemical inhibitors of caspases or genetic ablation of APAF1

(apoptosome formation) can prevent apoptosis induction even after MOMP.[32,33] While APAF1 was upregulated in *TP53*$^{+/+}$ and *TP53*$^{-/R248Q}$ cells after VenAza, increased PARP cleavage occurred only in *TP53*$^{+/+}$ cells (Figure 2A). This suggests disruption of an intermediate regulator between APAF1 and PARP cleavage in *TP53*$^{-/R248Q}$ cells.

Since the apoptosome (APAF1 and caspase-9 complex) activates executioner caspase-3/7 to cleave PARP, we asked whether dysfunction in caspase activation drives evasion of therapy-induced apoptosis. In a time-dependent manner, VenAza caused cleavage of initiator caspase-9 in both *TP53*$^{+/+}$ and *TP53*$^{-/R248Q}$ cells while executioner caspase-3 was cleaved selectively in *TP53*$^{+/+}$ cells (Figure 2F). Furthermore, caspase-9 and -3/7 activity was severely inhibited across all six isogenic *TP53*$^{-/mut}$ and *TP53*$^{-/-}$ MOLM-13 cells and *TP53*$^{-/-}$ MV-4-11 cells (Figure 2G-H). We reasoned that the lack of caspase-9 activity despite the presence of caspase-9 cleavage resulted in the loss of caspase-3 cleavage and activity in *TP53*$^{-/mut}$ cells.[34] VenAza induced increase in caspase-3/7 activity in *TP53*$^{+/+}$ cells in a time-dependent manner but remained unchanged in *TP53*$^{-/R248Q}$ cells (Figure S4D). We next evaluated whether reduced activation of caspase-3/7 in *TP53*$^{-/R248Q}$ and *TP53*$^{-/-}$ cells was due to defects in upstream caspase-8 activation via extrinsic signaling. While *TP53*$^{-/R248Q}$ and *TP53*$^{-/-}$ cells showed lower caspase-8 activity, the difference was less significant compared to changes in caspase-3/7 activation (Figure S4D-E). Since loss of mitochondrial membrane potential (MMP) during apoptosis may be impaired when caspases are dysfunctional,[35,36] we measured MMP in response to VenAza. *TP53*$^{-/R248Q}$ and *TP53*$^{-/-}$ cells had less tetramethylrhodamine ethyl ester (TMRE) fluorescence loss than *TP53*$^{+/+}$, emphasizing VenAza-induced caspase-9 and -3/7 dysfunction in *TP53* mutated cells (Figure S4F). Overall, these findings highlight that functional *TP53* is required for post-MOMP signaling to activate caspases and trigger VenAza-induced apoptosis in AML.

Unlike BH3 mimetics, chemotherapy relies on DNA damage rather than direct mitochondrial engagement to trigger MOMP, which is often impeded by *TP53* mutations. We next asked if *TP53* deficient solid cancers evade apoptosis through caspase inactivation. Across *TP53* deficient CRC and TNBC cells treated with standard of care chemotherapy, loss of caspase-3/7 activation was a conserved phenomenon (Figure 2H). However, *TP53* deficient CRC and TNBC cells showed upstream absence of MOMP post-chemotherapy, suggesting that stimuli for MOMP may be dependent on cell-specific determinants and *TP53* status (Figure S4G).

**_BIRC5_ deletion restores caspase activity in _TP53_ mutated AML**

We next searched for targetable dependencies that sensitize *TP53* mutated cells to apoptosis using genome-wide CRISPR knockout screening in $TP53^{+/+}$, $TP53^{-/R248Q}$, and $TP53^{-/-}$ isogenic MOLM-13 AML cells treated with DMSO or VenAza (Figure 3A). We utilized the Brunello library comprising 77,441 sgRNAs targeting 19,114 genes.[37] Comparison between $TP53^{+/+}$ isogenic MOLM-13 and parental MOLM-13 confirmed that clonal variability did not significantly affect functional dependency (Figure S5A). We identified that the top 100 VenAza sensitizing genes commonly shared across all genotypes were from the pro-apoptotic BCL-2 family, *BAX*, *PMAIP1* (NOXA), and *BCL2L11* (BIM) (Figure 3B and S5B). Since BH3-only proteins remained key sensitizers to VenAza despite *TP53* mutations, we next focused on genes involved in VenAza resistance and the apoptosis pathway. Using stringent filtering criteria, we first selected for 268 genes from in the Hallmark apoptosis and KEGG apoptosis gene sets from each genotype ($TP53^{+/+}$, $TP53^{-/R248Q}$, and $TP53^{-/-}$) before filtering for the top 100 hits, which narrowed down to a total of 7 resistance and 11 sensitizing genes (Figure S5C). *BCL2L1* (BCL-xL) was among the top scoring resistance genes in $TP53^{-/R248Q}$ and $TP53^{-/-}$ cells (Figure 3B and S5C). In $TP53^{-/R248Q}$

cells, *BIRC5* also stood out as resistant gene, since it encodes survivin, an inhibitor of apoptosis (IAP) family protein (Figure S5C). We next compared functional dependencies of *TP53*$^{-/R248Q}$ and *TP53*$^{-/-}$ cells against *TP53*$^{+/+}$ cells after VenAza treatment to determine the extent to which genes sensitize or confer resistance to *TP53* mutant or knockout cells relative to *TP53* wild-type cells in order to identify mutation-modulated treatment responses. We previously showed that *TP53*$^{-/R248Q}$ cells have increased BIM and BID levels despite presence of BAX downregulation and MCL-1 upregulation, which resulted in comparable MOMP with *TP53*$^{+/+}$ cells (Figure 2A-2C). Similarly, we identified that between VenAza treated cells, *TP53*$^{-/R248Q}$ and *TP53*$^{-/-}$ cells with BID or *BCL2L11* (BIM) knockout were enriched as compared to *TP53*$^{+/+}$ cells, indicating that the upregulation of BID and BIM indeed had a stronger influence in pushing these cells towards MOMP (Figure 3C). On the other hand, BAX, a sensitizing gene, was strongly enriched in *TP53*$^{+/+}$ cells, suggesting that BAX plays a stronger role to regulate MOMP in *TP53*$^{+/+}$ cells (Figure 3C). Interestingly, we found that the knockout of *BIRC5*, a gene conferring resistance, greatly induced cell death in both *TP53*$^{-/R248Q}$ and *TP53*$^{-/-}$ cells compared to *TP53*$^{+/+}$ cells (Figure 3C). We thus hypothesized that *BIRC5* deletion would overcome VenAza resistance in *TP53* mutated cells. Doxycycline (Doxy) inducible conditional genetic knockout of *BIRC5* (*BIRC5*-KO) sensitized *TP53*$^{-/R248Q}$, *TP53*$^{-/R175H}$, and *TP53*$^{-/R273H}$ cells to VenAza (Figure 3D). Since survivin may inhibit caspase activation through the HBXIP co-factor, we then investigated if caspase blockade in *TP53* mutated cells is *BIRC5*-dependent. Indeed, *BIRC5*-KO showed increased caspase-9 and -3/7 activity in *TP53*$^{-/R248Q}$, *TP53*$^{-/R175H}$, *TP53*$^{-/R273H}$, and *TP53*$^{+/+}$ cells treated with VenAza, highlighting the role of *BIRC5* in driving caspase inactivation (Figure 3E and S5D). Survivin encoded by *BIRC5* promotes XIAP stabilization by antagonizing the RING E3 ligase domain,[38] prompting us to evaluate involvement of other IAPs. We found that *BIRC5*-KO downregulated XIAP and c-IAP1 (Figure 3F). Although prior reports have shown that XIAP

may directly inhibit caspase-9 and caspase-3/7 activity,[39,40] however, deletion of *XIAP* (*XIAP*-KO) failed to restore caspase activity or trigger VenAza-induced cell death in *TP53*$^{-/R248Q}$ cells (Figure S5E). Moreover, *XIAP* overexpression did not protect *TP53*$^{+/+}$ cells from VenAza (Figure S5F). These findings convey that in *TP53* mutated AML, caspase inhibition is directly mediated by *BIRC5* rather than *XIAP*, suggesting that other IAPs may indirectly cooperate with *BIRC5* to regulate therapy-induced apoptosis in these cells.

**Wild-type *TP53* represses IAPs**

Having established BIRC5 dependency in TP53 mutated cells, we interrogated the regulatory relationship between *TP53* and *BIRC5*. We utilized nutlin-3a, an MDM2 antagonist that stabilizes p53 by disrupting p53-MDM2 interactions. We found that *TP53* stabilization by nutlin-3a decreased XIAP and survivin in *TP53*$^{+/+}$ cells but not *TP53*$^{-/R248Q}$ cells (Figure 3G). Next, to determine if p53-mediated suppression of *BIRC5* and *XIAP* occurred through direct promoter binding, we analyzed published chromatin-immunoprecipitation (ChIP-seq) data in isogenic MOLM-13 cells. However, we found no evidence of direct p53 binding to *XIAP* nor *BIRC5* promoters (Figure S5G).[23] RNA-seq in *TP53*$^{+/+}$, *TP53*$^{-/R248Q}$, and *TP53*$^{-/-}$ isogenic MOLM-13 AML cells treated with DMSO or VenAza revealed elevated *BIRC5* expression in both *TP53*$^{-/R248Q}$ and *TP53*$^{-/-}$ cells at baseline and after VenAza, which was further validated by RT-qPCR (Figure S5H-I). Our findings suggest that wild-type *TP53* may negatively regulate *BIRC5* in response to therapy-induced stress, a function lost upon *TP53* mutation.

**IAPs are upregulated in *TP53* mutated isogenic AML cells**

We next adopted global proteomics to identify determinants of VenAza resistance in *TP53* mutated AML. Data-independent acquisition (DIA) proteomics revealed distinct

clustering of untreated samples based on *TP53* status (*TP53*$^{+/+}$, *TP53*$^{-/R248Q}$, or *TP53*$^{-/-}$) (Figure S6A). Among apoptotic proteins, we observed significant downregulation of BAX and PUMA (*BBC3*) in *TP53*$^{-/R248Q}$ and *TP53*$^{-/-}$ cells compared to *TP53*$^{+/+}$ (Figure S6B). Notably, survivin and XIAP were significantly upregulated while BRUCE, another IAP family member, was downregulated (Figure 4A). Although BRUCE downregulation typically implies reduced degradation of caspase-9 and SMAC,[41] immunoblot analysis across *TP53*$^{-/mut}$ cells showed no such changes (Figure 4B). At baseline, *TP53* loss led to consistent upregulation of survivin, XIAP, and cIAP-1, while *TP53*$^{-/mut}$ cells showed variable expression compared to *TP53*$^{+/+}$ (Figure 4B). To extend these findings, we validated IAP (survivin, XIAP, cIAP-1) upregulation in additional *TP53*$^{-/-}$ cell lines: MOLM-13, MV-4-11, and HCT-116 (Figure 4C). Together, these findings provide powerful evidence that *TP53* mutated cells maintain elevated levels of IAPs that perhaps mediate apoptosis evasion.

**_BIRC5_ is upregulated in _TP53_ mutant human patient tumors**

To further explore clinical relevance of IAP upregulation in *TP53* mutated AML, we next turned to primary tumors. Investigation in published datasets, TCGA (14 *TP53*-mut versus 159 *TP53*-WT) and BeatAML (35 *TP53*-mut versus 404 *TP53*-WT), revealed that among IAPs, *BIRC5* was upregulated in *TP53*-mut tumors (Figure S6C). This expands on previous data showing *BIRC5* upregulation in various cancers, including AML.[42,43] To address limited sample size of *TP53* mutant patients in these cohorts, we next compared transcriptomic signatures in newly diagnosed AML patients (63 *TP53*-mut versus 668 *TP53*-WT) from the unpublished Munich Leukemia Laboratory (MLL) dataset. Consistent with TCGA and BeatAML studies, we observed downregulation of pro-death genes (*BAX*, *CASP2*, and *TP53*) and upregulation of anti-death genes (*MAPK1* and *PIK3R2*) (Figure 4D and S6D). *BIRC5* emerged as one of the most upregulated genes in *TP53*-mut tumors, consistent with

our findings in isogenic AML cell lines (Figure 4D-4E). Beyond AML, 17/25 different cancers from the TCGA cohort revealed *BIRC5* upregulation in TP53-mut tumors, underscoring a strong relationship with *BIRC5* (Figure 4F). Since *TP53* mutations often coincide with chromosome 17p loss, and *BIRC5* resides on chromosome 17q, we asked whether *BIRC5* upregulation was linked to chromosomal changes. We analyzed karyotype across 63 *TP53*-mut AML patients from the MLL dataset and found no significant difference in *BIRC5* expression when comparing 17p/17q chromosomal gains to losses, isolated 17p loss, or trisomy events affecting 17p/17q (Figure S7A). We next analyzed 17 cancers from the TCGA cohort that showed *BIRC5* upregulation in *TP53*-mutant tumors and selected 6 cancers with substantial 17p loss cases (*TP53*-mut > 100 patients, 17p loss > 50% patients). BRCA, STAD, and LUSC showed increased *BIRC5* levels when comparing 17p loss/17q gain to 17p loss/ 17q loss (Figure S7B). LUSC also exhibited significantly elevated *BIRC5* expression levels in cases with concurrent 17p loss and 17q gain compared to those displaying isolated 17p loss, isolated 17q gain, or karyotypically intact chromosome 17 (Figure S7B). Our findings indicate that genomic instability may contribute to *BIRC5* upregulation in specific *TP53*-mut cancers.

To interrogate survivin upregulation at the protein level, we performed RPPA in primary AML tumors. Survivin expression levels were significantly elevated in *TP53*-mut tumors relative to *TP53*-WT tumors, and in complex-karyotype tumors (defined as >3 chromosomal abnormalities) compared to non-complex karyotypes (Figure 4G). Enrichment of survivin was not observed in *FLT3*, *IDH1/2*, *NPM1*, and *RUNX1* mutant patients (Figure S7C). As expected and previously reported, *TP53* mutant AML patients had significantly worse survival outcomes compared to wild-type patients (Figure S7D). Next, we stratified AML patients by *BIRC5* expression level. Elevated *BIRC5* level in AML patients resulted in

poor survival outcomes (Figure 4H). Importantly, these findings establish *BIRC5* upregulation as a compelling therapeutic target across multiple *TP53* mutated tumors.

**Unbiased drug screening identifies survivin and IAP inhibitors as actionable therapy for *TP53* mutant tumors**

To identify therapeutic vulnerabilities in *TP53* mutated cells, we applied an unbiased high-throughput drug screening approach. We screened 289 clinically relevant agents, where a majority of them are FDA-approved or in Phase II/III trials, against isogenic $TP53^{+/+}$, $TP53^{-/R248Q}$, and $TP53^{-/-}$ MOLM-13 cells (Figure 5A). We combined VenAza at the $TP53^{+/+}$ IC50 concentration with each third agent at 10 nM and 1000 nM (Figure S8A). Screen quality was validated, as demonstrated by the consistency between replicates, where correlation coefficients were greater than 0.95, emphasizing the reliability of our results (Figure S8B). Notably, $TP53^{-/R248Q}$ cells showed reduced drug sensitivity compared $TP53^{+/+}$ cells, with fewer agents scoring at both 10 nM (16 versus 18) and 1000 nM (54 versus 95) (Figure 5B and S8C). Reduced sensitivity in $TP53^{-/R248Q}$ cells aligns with clinical observations of *TP53* mutations conferring resistance to conventional treatments. Since we had multiple drugs targeting similar pathways, we grouped all 289 agents according to their drug class to determine if agents from same drug class had similar efficacy at 10 nM. We identified that drugs targeting apoptosis, cell cycle regulators, and receptor kinase pathway modulators were prominent clusters, showing consistent strong response across all genotypes (Figure 5C and S8D-E).

We next examined drug sensitivity patterns to search for agents with selective activity by *TP53* status. We selected the top 10% of scored agents from each genotype and identified that the majority (22/29 agents) scored in all genotypes, suggesting that effectiveness of these drugs transcends the influence of *TP53* status (Figure 5D). Daunorubicin and idasanutlin

scored selectively in *TP53*$^{+/+}$ cells, confirming their dependence on functional *TP53* for anti-tumor activity (Figure 5D).[44] Z-score analysis comparing *TP53*$^{-/R248Q}$ and *TP53*$^{-/-}$ cells to *TP53*$^{+/+}$ cells consistently scored survivin (sepantronium bromide, NSC-80467) and IAP (birinapant, AZD5582) inhibitors in *TP53*$^{-/R248Q}$ and *TP53*$^{-/-}$ cells, incriminating IAPs as key drivers of therapy-induced resistance (Figure 5B and S8C). Additional hits included inhibitors of HDAC (quisinostat, panobinostat), cell cycle (dinaciclib, prexasertib, filanesib), and apoptosis (MCL-1 targeters: S63845) (Figure 5B, 5D, S8C, and 8E). To investigate monotherapy efficacy for identified top hits in *TP53* mutated cells, we performed validation screening at seven-point concentrations. This validation screening uncovered thirteen drugs with IC50 <20 nM, including survivin and IAP inhibitors (Figure S8F). Among these, birinapant demonstrated superior synergy in combination with VenAza (Figure 5E). Together, both our CRISPR and drug screens converged on survivin and IAPs as potentially targetable dependencies in *TP53* mutated AML to evade therapy-induced apoptosis.

**Survivin and IAP inhibitors restore sensitivity to VenAza in *TP53* mutated AML**

Having identified survivin (sepantronium bromide, NSC-80467) and IAP (birinapant, AZD5582) inhibitors as top hits from the drug screen, we next investigated their therapeutic potential in *TP53* mutated AML. As single agents, AZD5582, birinapant, sepantronium bromide, and NSC-80467 were potent to *TP53*$^{-/R248Q}$ and *TP53*$^{-/-}$ cells (Figure S9A). The efficacy of birinapant extended to five additional isogenic AML cell lines harboring different *TP53* mutations (Figure S9B). Notably, combination of birinapant with VenAza (VenAza-Bir) led to >10-fold reduction in Ven IC50 in *TP53*$^{-/R248Q}$ and led to robust apoptosis induction across all three genotypes (Figure 6A-B and S9C). Addition of NSC-80467 likewise restored VenAza sensitivity in both *TP53*$^{-/R248Q}$ and *TP53*$^{-/-}$ cells (Figure S9D).

Since *TP53* mutated AML showed block in caspase activation, we next tested whether IAP inhibitors mechanistically restored sensitivity by reactivating caspases. Birinapant treatment reduced XIAP and cIAP-1 levels in *TP53*$^{+/+}$ and *TP53*$^{-/R248Q}$ cells (Figure 6C). In *TP53*$^{-/R248Q}$ cells, birinapant increased cleaved caspase-9, -3/7, and PARP with corresponding increase in caspase-3/7 activity, which VenAza alone had a limited effect (Figure 6C-D). Additionally, birinapant triggered loss in mitochondrial membrane potential in *TP53*$^{+/+}$, *TP53*$^{-/R248Q}$, and *TP53*$^{-/-}$ cells, indicating restored caspase-9 and -3/7 activity (Figure S9E). Since survivin regulates both apoptosis and cell division, we then asked whether survivin inhibitors restore VenAza sensitivity through apoptotic pathways. Both survivin inhibitors, NSC-80467 and sepantronium bromide, enhanced caspase-3/7 activity in *TP53*$^{+/+}$, *TP53*$^{-/R248Q}$, and *TP53*$^{-/-}$ cells (Figure S9F). Sepantronium bromide increased Annexin V/PI staining and a higher proportion of cells in the sub-G1 phase, both indicative of elevated apoptosis levels (Figure S9G-H). These findings demonstrate that survivin and IAP inhibitors overcome therapy resistance in *TP53* mutated AML by restoring caspase-dependent apoptosis.

**Survivin inhibitors overcome chemotherapy resistance in *TP53* deficient solid cancers**

To explore the broader therapeutic potential of survivin and IAP inhibitors, we investigated their efficacy in *TP53* deficient CRC and TNBC cells. Survivin inhibitors showed enhanced potency in *TP53*$^{-/-}$ HCT-116 and CAL-51 compared to *TP53*$^{+/+}$ (Figure S10 A). Furthermore, addition of survivin inhibitors restored chemosensitivity to 5-FU and doxorubicin (Figure S10B). In contrast to AML, birinapant, an IAP inhibitor, failed to enhance chemotherapy efficacy in *TP53*$^{-/-}$ HCT-116 and CAL-51 cells (Figure S10C). This highlights survivin inhibitors as a class of agents that may be effective in multiple *TP53* mutated cancers beyond AML.

Having found reduction in caspase activity in TP53 deficient CRC and TNBC, we investigated the mechanism of survivin inhibitor efficacy. Surprisingly, the cytotoxic effects of sepantronium bromide and NSC-80467 occurred independent of caspase restoration (Figure S10D). Hence, we next measured cell cycle profiles and found minimal sub-G1 accumulation post-treatment (<5%) but prominent G2/M accumulation, consistent with mitotic arrest (Figure S10E). These findings demonstrate that survivin inhibitors mediate sensitization in *TP53* mutated tumors via distinct paths: caspase restoration in AML and mitotic arrest in solid tumors. Despite these tissue-specific mechanisms, Survivin inhibitors consistently overcame both chemotherapy and targeted therapy resistance across different tumor types. This provides compelling rationale for combining standard of care drugs with Survivin inhibitors to resensitize *TP53* mutant cancers.

**Survivin and IAP inhibitors cause leukemia inhibition *in vivo***

To validate therapeutic efficacy *in vivo*, we treated $TP53^{+/+}$ and $TP53^{-/R248Q}$ AML xenografts with VenAza-Bir or VenAza and sepantronium bromide (VenAza-Sep) (Figure 6E and S11A). Clinically, VenAza is standard of care for AML patients irrespective *TP53* status. Since *TP53* mutant patients perform poorly on VenAza, we first tested *in vivo* efficacy of VenAza-Bir at 5 days post-engraftment. VenAza-Bir was superior in $TP53^{-/R248Q}$ mice (median 44.5 days) compared to single agent birinapant (median 19 days) or VenAza alone (median 26 days) in $TP53^{+/+}$ mice (Figure S11B). We further tested VenAza-Bir efficacy in a more clinically relevant setting with treatment delayed until 15 days post-engraftment (when mice displayed partial hind-limb paralysis from tumor burden). With delayed time to treatment, $TP53^{-/R248Q}$ mice showed rapid leukemia progression on VenAza. However, VenAza-Bir significantly reduced circulating blasts and demonstrated superior tumor suppression in spleen and bone marrow compared to VenAza alone in both genotypes (Figure

6F). This translated to improved survival in *TP53*$^{-/R248Q}$ mice receiving VenAza-Bir (median 33 days) versus VenAza alone (22 days) or VenAza in *TP53*$^{+/+}$ mice (27 days) (Figure 6G).

VenAza-Sep also showed comparable anti-leukemic efficacy in *TP53*$^{-/R248Q}$ mice across peripheral blood and spleen compartments but limited activity in bone marrow (Figure S11C). Since sepantronium bromide has short plasma half-life (approximately 1-2 hours),[45] we speculate limited distribution of drug to the bone marrow compartment. *TP53*$^{-/R248Q}$ mice treated with VenAza-Sep had greater survival (median 27 days) over VenAza alone in *TP53*$^{-/R248Q}$ mice (median 22 days), which was equal to VenAza alone in *TP53*$^{+/+}$ mice (median 27 days) (Figure S11D). All treatments were well-tolerated, with mice receiving VenAza-Bir maintaining body weights comparable to those on VenAza alone (Figure S11E). Furthermore, histological assessment of various organs from *TP53*$^{-/R248Q}$ mice following 6-weeks of VenAza-Bir treatment showed selective effects in bone marrow and spleen and preservation of healthy tissue in the lung, liver, heart, and kidney (Figure S11F). Collectively, survivin and IAP inhibitors were effective therapeutic partners for standard of care therapy in *TP53* mutated AML.

### ***TP53* mutant patient HSC/MPP single cells have elevated *BIRC5***

To investigate the clinical significance of BIRC5 expression in therapy resistance, we performed single-cell RNA-seq on paired diagnostic and relapse (with and without venetoclax-based combination therapy) samples from 22 AML patients – of which 7 are TP53 mutated and 15 did not have TP53 mutation (Figure 7A). Cell types were annotated based on established lineage-specific gene markers and leukemic blast cells (malignant) were distinguished from non-malignant cells (Figure 7A). Removing non-malignant cells, initial analysis at diagnosis revealed that a unique cellular composition of BIRC5 expressing cells. Specifically, BIRC5 is commonly expressed in the erythroid cells (pink, orange, dark

orange), pDC cells (teal), and in hematopoietic stem cells and multipotent progenitor cells (HSC/MPP) (Figure 7A and S12A).

Longitudinal analysis of patients treated with venetoclax-based combination therapy revealed that *TP53* wild-type patients demonstrated therapeutic efficacy through marked reduction in HSC/MPP populations, while a significant portion of HSC/MPPs remained in *TP53* mutant patients post treatment (Figure 7B and S12B). Notably, expansion in monocytic cell populations was observed in *TP53* wild-type patients and in T and NK cell populations in *TP53* mutant patients (Figure 7B and S12B). Strikingly, within the HSC/MPP cell populations, cells from TP53 mutant patients saw an increase in BIRC5 expressing cells and BIRC5 expression post treatment (Figure 7C-D). These findings not only establish BIRC5 as a characteristic feature of TP53 mutant tumors but also identify BIRC5-high cells as key mediators of venetoclax resistance in both wild-type and TP53 mutant contexts. Given that TP53 mutated AML patients historically respond poorly to standard of care VenAza, these discoveries provide a new biological understanding and treatment options for this highly-resistant subgroup of AML patients.

## DISCUSSION

Therapy resistance remains a significant roadblock to cancer cure in *TP53* mutated tumors despite understanding tumorigenic mechanisms. Ominously, AML patients with *TP53* mutations demonstrate upfront resistance towards both conventional chemotherapy and VenAza therapy.[1–3,8–11] Moreover, genetic screening in AML cell lines has linked venetoclax resistance to *TP53* loss.[46–48] Here, we report that addition of survivin and IAP inhibitors to VenAza outperformed leukemia inhibition *in vivo* compared to VenAza alone in *TP53* mutated and wild-type xenografts. These findings have massive translational significance

since *TP53* mutant AML patients relapse on VenAza in <6 months, and recent clinical trials with eprenetapopt (p53 activator) plus azacitidine (hypomethylator) and magrolimab (anti-CD47 antibody) plus azacitidine have been met with disappointment.[49–52]

While prior studies have focused on activating canonical wild-type *TP53* target genes via *TP53* activators to overcome therapy resistance,[53,54] we alternatively explored *TP53* functions beyond transactivation. *TP53* mutations caused loss of numerous pro-apoptotic targets, yet BIM-EL upregulation in AML and solid cancers implied revival of apoptotic signaling. Indeed, our study highlights the previously unreported discovery that MOMP is not the point of no return for *TP53* mutant tumors to evade therapy-induced apoptosis. Furthermore, we identified that wild-type *TP53* is required for post-MOMP caspase activation. Caspase inactivation was a conserved multi-cancer mechanism of resistance for tumors with homozygously deleted *TP53* (AML, CRC, and TNBC), regardless of chemotherapy or targeted therapy. While most studies have focused on *TP53* deletions, there is emerging evidence that *TP53* mutations also show distinct phenotypes and clinical outcomes.[55] Across our six different *TP53* missense mutations in AML, caspase blockade was a conversed phenomenon to evade therapy-induced apoptosis.

Beyond transactivation, *TP53* negatively regulates many targets,[23,39,56,57] but whether one target stands out from the rest as the core driver of therapy resistance following mutation had been undefined. By whole-genome CRISPR screen, we unveiled *BIRC5* (survivin) as one such functional dependency of *TP53* mutated AML to evade therapy-induced apoptosis. While *BIRC5* overexpression in cancer tissues has been recognized,[58] we show that genomic heterogeneity drives differential *BIRC5* expression. Across different AML-associated recurrent gene mutations (*FLT3, IDH2, NPM1, RUNX1*), only *TP53* mutations and complex karyotypes conferred *BIRC5* upregulation. More broadly, in >100 *TP53* mutated AML primary tumors and 18 additional tumor types from the TCGA cohort, *BIRC5* upregulation

was consistently observed. In AML, *BIRC5* deletion restored caspase-9 and -3/7 activity and downregulated other IAPs, highlighting a relationship between survivin and caspases. Although survivin is classified as an IAP, whether it is directly inhibiting caspases remains controversial due to lack of a C-terminal ring finger domain.[40,59] Some studies suggested that survivin inhibits caspases by indirect binding of caspase-9 through stabilization of XIAP, by direct binding of Survivin-HBXIP complex to procaspase-9 to prevent binding to APAF1, or by antagonizing SMAC.[59]

We identified *BIRC5* as a targetable vulnerability to overcome therapy resistance in *TP53* mutant tumors (Figure 7E). That being said, our findings reveal that mechanisms of cytotoxicity following survivin inhibition may vary by tumor type. In *TP53* mutated AML, where cells are inherently primed for apoptosis, survivin primarily functions as an IAP to block caspases. Consequently, survivin inhibition overcomes VenAza resistance primarily by restoring caspase activity to induce apoptosis. In contrast, *TP53* deficient solid tumors, which are less apoptotically primed, response to survivin inhibition might be via G2/M arrest and subsequent mitotic catastrophe rather than caspase reactivation. Furthermore, the vulnerability to G2/M transition modulators in *TP53* mutated cells extends beyond survivin – our drug screen identified additional effective agents targeting this phase, including aurora-B kinase inhibitor, barasertib, and kinesin spindle protein inhibitor, filanesib. This sensitivity likely emerges because *TP53* mutated cells, while able to bypass G1/S checkpoints, become increasingly dependent on mitotic regulators by upregulating survivin for successful cell division.

Nevertheless, survivin's unique dual role in both apoptosis and mitosis makes it a particularly promising therapeutic target. Our longitudinal single-cell RNA sequencing analysis revealed selective enrichment of *BIRC5* expression within therapy-resistant HSC/MPP populations following venetoclax-based treatment, implying *TP53* mutation status

can guide patient stratification and rational implementation of survivin/IAP inhibitor therapy. However, several questions remain, including whether different *TP53* mutations preferentially rely on either anti-apoptotic or mitotic functions of survivin and how different co-mutations and varying degrees of genomic instability might influence these functional dependencies. Regardless, our findings provide compelling rationale for clinical investigation of survivin and IAP inhibitors, as well as other agents targeting survivin's diverse functions in *TP53* mutated cancers.

**Statement of Contributions**

S.B. conceptualized the study, designed the experiments, and wrote the manuscript. A.M.M. and F.Q.L. conceptualized and designed experiments, designed figures, performed experiments, analyzed data, and wrote the manuscript; both authors contributed equally. Y.M. performed high-throughput drug screening and validation in isogenic AML cell lines. E.A.O. designed figures and wrote the manuscript. C.G.T.C., Y.W., J.Y.M.T., and K.S.B. performed experiments and analyzed data. S.J. performed BH3 profiling and DBP experiments and analyzed data. X.X.L. and A.N.M. analyzed and plotted data. V.S. performed proteomics experiments, analyzed data, and critically reviewed the manuscript. C.W. generated *TP53* knockout AML cell lines. P.M. performed mass spectrometry proteomics and analyzed data. L.H. designed BH3 profiling experiments. B.D.B. and S.M.K. designed survival experiments, measured survivin levels in the MD Anderson patient dataset, and analyzed data. T.H. provided bulk transcriptomic analysis of the MLL patient dataset. R.C.L. provided samples for BH3 profiling and sequenced *TP53* status from DFCI patients. A.P. supervised and analyzed bulk RNA-seq in isogenic AML cell lines. A.L. supervised and guided BH3 profiling experiments and critically reviewed the manuscript. J.K. designed and supervised experiments, analyzed proteomics data, and critically reviewed the manuscript. E.A. analyzed

single cell and bulk data from the MLL dataset and MD Anderson Moon Shots dataset. K.I. provided expertise regarding acquisition of *BIRC5* upregulation and critically reviewed the manuscript. M.A. supervised experiments on the MD Anderson dataset, provided patient samples, and contributed to single cell/bulk RNA-seq and proteomics experiments.

## MATERIALS AND METHODS

A detailed description of experimental methods, including alkaline comet assay, animal studies, beta-galactosidase senescence assay, BH3 profiling, dynamic BH3 profiling, caspase luminescence assay, cell culture, cell cycle/apoptosis and viability studies, clonal competition assay, colony forming assay, CRISPR library screen, cytotoxicity assay, data-independent acquisition (DIA) proteomics, drug library screen, generation of knockout and overexpression cells, patient cohorts, reverse phase protein array, RT-qPCR, RNA-seq, scRNQ-seq, TMRE staining, and western blotting/coimmunoprecipitation, can be found in the supplement.

### Statistical significance

Calculation of statistical significance was conducted using two-tailed t-tests unless otherwise specified. Proteomics analysis via two-sided t-test adjusted with Benjamini-Hochberg method. One-tailed Wilcoxon test to assess MLL, BeatAML and TCGA datasets and differential survivin protein expression between mutant vs non-mutant *TP53* or complex vs non-complex karyotype in clinical samples. Differences in cumulative survival probability was determined by Kaplan-Meier Analysis. Caspase assay: Calculation of statistical significance was conducted using two-tailed t-tests. For all figures, *$p<0.05$, **$p<0.01$, ***$p<0.001$, ****$p<0.0001$.

## Figure Legends

**Figure 1. *TP53* mutated isogenic AML cells have reduced apoptosis and viability in response to standard therapy.**

**(A)** Schematic for functional analysis of *TP53* AML (MOLM-13, MV-4-11), CRC (HCT-116), and TNBC (CAL-51) cells. **(B)** Cell viability of *TP53* active (EV, WT) and knockout (sg1, sg2, KO) cells treated with standard of care chemotherapy for 72 hours: AML (MOLM-13, MV-4-11) with Ven and 50 nM Aza, CRC (HCT-166) with 5-FU, and TNBC (CAL-51) with doxorubicin (Dox). **(C)** Representative images of colony formation assays showing increased growth of MOLM-13 $TP53^{-/R248Q}$ cells treated with DMSO or VenAza for 72 hours in RPMI followed by 9 days in Methocult. Colony forming units were normalized to respective DMSO treated cells. **(D)** Clonal competition assay showed that $TP53^{-/R248Q}$ and $TP53^{-/-}$ cells have competitive advantage compared to $TP53^{+/+}$ cells when treated with VenAza for 10 days. **(E-F)** Annexin V and PI or DAPI assay demonstrated greater viable cell populations in *TP53* mutated cells: **(E)** MOLM-13 with VenAza, cytarabine (200 nM), or etoposide (200 nM); **(F)** MV-4-11 with VenAza, CAL-51 with doxorubicin (50 nM), and HCT-116 with 5-FU (50 μM). **(G)** Alkaline comet assay of $TP53^{+/+}$ and $TP53^{-/R248Q}$. MOLM-13 cells treated with DMSO or 1 nM Ven and 50 nM Aza for 7 days reveals increased tail moment in *TP53* mutated cells. See Figure S2 for quantification. For all figures unless otherwise specified, treatment with VenAza: venetoclax 3 nM, azacitidine 50 nM.

**Figure 2. *TP53* mutated AML cells fail to activate caspases despite MOMP induction in response to therapy.**

**(A)** Immunoblotting of BH3 family proteins and other apoptotic factors in *TP53*$^{+/+}$ and *TP53*$^{-/R248Q}$ cells treated with DMSO or VenAza for 24 hours. **(B)** Coimmunoprecipitation assay identifying interactions between BIM:MCL-1 or BIM:BCL-2. **(C)** Baseline BH3 profiling heatmap showing mitochondrial priming response of DMSO and titrated BIM for AML (MOLM-13 *TP53*$^{+/+}$, *TP53*$^{-/mut}$, *TP53*$^{-/-}$, and MV-4-11), CRC (HCT-116), and TNBC (CAL-51) cells. BIM concentrations used: MOLM-13 *TP53*$^{+/+}$, *TP53*$^{-/mut}$, *TP53*$^{-/-}$: 0.03-3.0 μM; MV-4-11: 0.1-0.5 μM; HCT-116 and CAL-51: 0.1-1.0 μM. Dagger = decreased priming. Asterisk = increased priming. **(D)** BH3 profiles for BIM peptide and venetoclax as a peptide in primary AML samples based on *TP53* status. **(E)** Dynamic BH3 profiling heatmap after treating MOLM-13 isogenic cells AML (*TP53*$^{+/+}$, *TP53*$^{-/mut}$, *TP53*$^{-/-}$) for 4 hours with VenAza (1 nM Ven and 50 nM Aza). Dagger = decreased priming. Asterisk = increased priming. **(F)** Western blot of cleaved caspase-9, cleaved caspase-3 and total caspase-3 after treatment of MOLM-13 *TP53*$^{+/+}$ and *TP53*$^{-/R248Q}$ with VenAza across different timepoints. **(G-H)** Caspase-3/7 and caspase-9 activity measured in AML cells after 24 hours of VenAza, CRC cells after 24 hours of 5-FU (50 μM), and TNBC cells after 48 hours of doxorubicin (Dox, 50 nM).

**Figure 3. Mutated *TP53* cell lines have upregulated *BIRC5*.**

**(A)** Schematic of CRISPR screen for identifying sensitizing and resistance genes. **(B)** CRISPR screen for *TP53*$^{+/+}$, *TP53*$^{-/R248Q}$, and *TP53*$^{-/-}$ MOLM-13 cells treated with VenAza and DMSO. Sensitize refers to genes that conferred higher killing (enriched sgRNA guides after VenAza) and resistance refers to genes that conferred survival (depleted sgRNA guides after VenAza). Cut-off was pre-determined by MAGeCKFlute, where cutoff scores for *TP53*$^{+/+}$, *TP53*$^{-/R248Q}$, and *TP53*$^{-/-}$ were ±2.466, ±1.328 and ±1.738 respectively. **(C)** CRISPR screen for *TP53*$^{-/R248Q}$ and *TP53*$^{-/-}$ against *TP53*$^{+/+}$ MOLM-13 cells treated with VenAza. **(D-E)** Cell viability and caspase-3/7 and -9 activity for *TP53*$^{-/R248Q}$, *TP53*$^{-/R175H}$, and *TP53*$^{-/273H}$ cells with *BIRC5*-KO after 72 hours of treatment with doxycycline (10 ng), VenAza (Ven 3 nM, Aza 50 nM), or combination. Data normalized to respective DMSO-treated cells. **(F)** Western blot for indicated proteins with *BIRC5*-KO (Doxy +) and *XIAP*-KO (Doxy +). **(G)** Western blot shows nutlin-3a (5 μM for 24 hours) downregulated surviving and XIAP selectively in MOLM-13 *TP53*$^{+/+}$ but not *TP53*$^{-/R248Q}$ cells.

**Figure 4. Primary AML tumors and isogenic cells with *TP53* mutations have upregulated *BIRC5*.**

**(A)** Scatterplot of data-independent acquisition (DIA) proteomics of isogenic MOLM-13 cells at the baseline. Protein expression in *TP53*$^{-/R248Q}$ and *TP53*$^{-/-}$ were compared to *TP53*$^{+/+}$ cells. Blue: pro-apoptotic proteins; green: anti-apoptotic proteins; red: inhibitor of apoptosis proteins. Analysis via two-sided t-test adjusted with Benjamini-Hochberg method. **(B)** Western blot showing baseline protein expression in *TP53*$^{+/+}$, *TP53*$^{-/mut}$, and *TP53*$^{-/-}$ MOLM-13 cells. **(C)** Western blot showing baseline protein expression in *TP53*$^{+/+}$ or *TP53*$^{-/-}$ MOLM-13, MV-4-11, and HCT-116 cell lines. **(D)** mRNA levels of selected apoptosis genes in AML primary tumor cohort from the Munich Leukemia Laboratory dataset demonstrating significant differences in gene expression in *TP53*-mut AML relative to *TP53*-WT AML. **(E)** Expression level of *BIRC5* mRNA in primary AML patients from the Munich Leukemia Laboratory stratified by *TP53* status. **(F)** Upregulation of *BIRC5* mRNA obtained from RNA-seq of individual patients across multiple cancers from the TCGA database in 17 of 26 cancers. Analysis via Wilcoxon test. **(G)** Survivin protein levels measured via RPPA in AML patients stratified by *TP53* status or karyotype. **(I)** Kaplan-Meier survival plots for groups stratified according to survivin expression levels.

**Figure 5. High-throughput drug screening identifies Survivin and IAP inhibitors as combination partners for sensitizing *TP53* mutated cells to VenAza.**

**(A)** Schematic of high-throughput drug screening in MOLM-13 $TP53^{+/+}$, $TP53^{-/R248Q}$, and $TP53^{-/-}$ cells treated with venetoclax (3 nM) and azacitidine (50 nM), with a third agent from a drug library of 289 agents. The third agent is added at concentrations of 10 nM or 1000 nM. Agents with z-score > 2 were selected. **(B)** Z-score correlation scatterplots comparing z-scores of agents at 10 nM, with comparisons between $TP53^{-/R248Q}$ vs $TP53^{+/+}$, $TP53^{-/-}$ vs $TP53^{+/+}$, and $TP53^{-/R248Q}$ vs $TP53^{+/+}$. Z-score cut-off > 2 across all genotypes. **(C)** Cell viability heatmap of all agents clustered by target pathway at 10 nM concentration. **(D)** Venn diagram presenting the top 10% of scored agents from each genotype treated at 10 nM. Z-score cut-off for $TP53^{+/+}$, $TP53^{-/R248Q}$, and $TP53^{-/-}$ cells were 4.34, 3.71, and 4.72 respectively. **(E)** Synergy scores revealed that birinapant synergizes strongly with VenAza in $TP53^{+/+}$, $TP53^{-/R248Q}$, and $TP53^{-/-}$ MOLM-13 cells.

**Figure 6. Survivin and IAP inhibitors restore caspase activation leading to apoptosis in mutated *TP53* AML cells and *in vivo* leukemia inhibition.**

**(A)** Cell viability of isogenic MOLM-13 $TP53^{+/+}$ and $TP53^{-/R248Q}$ cells treated with Ven, 50 nM Aza, and 20 nM birinapant for 72 hours. **(B)** Annexin V-APC and PI assay showed increased cell death populations in $TP53^{+/+}$ and $TP53^{-/R248Q}$ cells treated with VenAza, birinapant, and VenAza plus birinapant (10 nM or 20 nM) for 72 hours. **(C)** Western blot presenting reduced XIAP and cIAP-1 with increased cleaved caspase-9 and -3 after treatment with birinapant (20 nM) for 24 hours. **(D)** Caspase-3/7 activity in isogenic MOLM-13 cells treated with DMSO, VenAza, birinapant (20 nM), or VenAza-Bir for 24 hours. **(E)** Schematic of *in vivo* study where NSG mice (n = 30) were engrafted with either isogenic MOLM-13 $TP53^{+/+}$ or $TP53^{-/R248Q}$ cells. At 15 days post-transplant, mice were further split into six groups and were treated with either vehicle, VenAza, or VenAza-Bir. **(F)** Blast count percentages were reduced in the peripheral blood of mice 4 days and 11 days post-treatment with birinapant. Blast count percentages in spleen and bone marrow were reduced at the end point. **(G)** Survival percentage of mice by treatment group.

**Figure 7. The proportion of *TP53* mutated cells expressing *BIRC5* increases in AML patients after relapse on venetoclax.**

**(A)** UMAP plot visualizing the distribution of single cells based on their hematopoietic and leukemic subpopulations. **(B)** Proportion of cells treated with venetoclax expressing *BIRC5* (defined as *BIRC5* gene expression > 0) in various cell subpopulations between two timepoints (diagnosis, Dx and post-treatment, Post-tx) stratified by *TP53* mutation status. **(C)** Sankey diagram illustrating the shift in percentage distribution of various cell subpopulations treated with venetoclax between two time points, Dx and Post-tx, stratified by *TP53* mutation status. **(D)** Expression levels of *BIRC5* in HSC/MPP cell subpopulations treated with venetoclax between two timepoints, Dx and Post-tx, stratified by *TP53* mutation status. **(E)** Schematic of *TP53* mutated AML evading apoptosis due to *BIRC5* upregulation mediated caspase inactivation and resensitizing them by inhibitors of survivin and IAPs.

## REFERENCES


1. Toma-Jonik A, Vydra N, Janus P, Widłak W. Interplay between HSF1 and p53 signaling pathways in cancer initiation and progression: non-oncogene and oncogene addiction. *Cell Oncol Dordr*. 2019;42(5):579-589. doi:10.1007/s13402-019-00452-0

2. Kastenhuber ER, Lowe SW. Putting p53 in Context. *Cell*. 2017;170(6):1062-1078. doi:10.1016/j.cell.2017.08.028

3. Barbosa K, Li S, Adams PD, Deshpande AJ. The role of TP53 in acute myeloid leukemia: Challenges and opportunities. *Genes Chromosomes Cancer*. 2019;58(12):875-888. doi:10.1002/gcc.22796

4. Papaemmanuil E, Gerstung M, Bullinger L, et al. Genomic Classification and Prognosis in Acute Myeloid Leukemia. *N Engl J Med*. 2016;374(23):2209-2221. doi:10.1056/NEJMoa1516192

5. Lindsley RC, Saber W, Mar BG, et al. Prognostic Mutations in Myelodysplastic Syndrome after Stem-Cell Transplantation. *N Engl J Med*. 2017;376(6):536-547. doi:10.1056/NEJMoa1611604

6. Feurstein S, Rücker FG, Bullinger L, et al. Haploinsufficiency of ETV6 and CDKN1B in patients with acute myeloid leukemia and complex karyotype. *BMC Genomics*. 2014;15(1):784. doi:10.1186/1471-2164-15-784

7. Pollyea DA, Pratz KW, Wei AH, et al. Outcomes in Patients with Poor-Risk Cytogenetics with or without TP53 Mutations Treated with Venetoclax and Azacitidine. *Clin Cancer Res Off J Am Assoc Cancer Res*. 2022;28(24):5272-5279. doi:10.1158/1078-0432.CCR-22-1183

8. DiNardo CD, Pratz K, Pullarkat V, et al. Venetoclax combined with decitabine or azacitidine in treatment-naive, elderly patients with acute myeloid leukemia. *Blood*. 2019;133(1):7-17. doi:10.1182/blood-2018-08-868752

9. Konopleva M, Letai A. BCL-2 inhibition in AML: an unexpected bonus? *Blood*. 2018;132(10):1007-1012. doi:10.1182/blood-2018-03-828269

10. Wei AH, Strickland SA, Hou JZ, et al. Venetoclax Combined With Low-Dose Cytarabine for Previously Untreated Patients With Acute Myeloid Leukemia: Results From a Phase Ib/II Study. *J Clin Oncol Off J Am Soc Clin Oncol*. 2019;37(15):1277-1284. doi:10.1200/JCO.18.01600

11. DiNardo CD, Jonas BA, Pullarkat V, et al. Azacitidine and Venetoclax in Previously Untreated Acute Myeloid Leukemia. *N Engl J Med*. 2020;383(7):617-629. doi:10.1056/NEJMoa2012971

12. Kim K, Maiti A, Loghavi S, et al. Outcomes of TP53-mutant acute myeloid leukemia with decitabine and venetoclax. *Cancer*. 2021;127(20):3772-3781. doi:10.1002/cncr.33689

848 13. Daver N, Wei AH, Pollyea DA, Fathi AT, Vyas P, DiNardo CD. New directions for
849 emerging therapies in acute myeloid leukemia: the next chapter. *Blood Cancer J*.
850 2020;10(10):107. doi:10.1038/s41408-020-00376-1

851 14. Green DR, Kroemer G. Cytoplasmic functions of the tumour suppressor p53. *Nature*.
852 2009;458(7242):1127-1130. doi:10.1038/nature07986

853 15. Yu J, Wang Z, Kinzler KW, Vogelstein B, Zhang L. PUMA mediates the apoptotic
854 response to p53 in colorectal cancer cells. *Proc Natl Acad Sci U S A*. 2003;100(4):1931-
855 1936. doi:10.1073/pnas.2627984100

856 16. Oda E, Ohki R, Murasawa H, et al. Noxa, a BH3-only member of the Bcl-2 family and
857 candidate mediator of p53-induced apoptosis. *Science*. 2000;288(5468):1053-1058.
858 doi:10.1126/science.288.5468.1053

859 17. Miyashita T, Harigai M, Hanada M, Reed JC. Identification of a p53-dependent negative
860 response element in the bcl-2 gene. *Cancer Res*. 1994;54(12):3131-3135.

861 18. Wu Y, Mehew JW, Heckman CA, Arcinas M, Boxer LM. Negative regulation of bcl-2
862 expression by p53 in hematopoietic cells. *Oncogene*. 2001;20(2):240-251.
863 doi:10.1038/sj.onc.1204067

864 19. Chipuk JE, Kuwana T, Bouchier-Hayes L, et al. Direct activation of Bax by p53 mediates
865 mitochondrial membrane permeabilization and apoptosis. *Science*. 2004;303(5660):1010-
866 1014. doi:10.1126/science.1092734

867 20. Chipuk JE, Bouchier-Hayes L, Kuwana T, Newmeyer DD, Green DR. PUMA couples
868 the nuclear and cytoplasmic proapoptotic function of p53. *Science*.
869 2005;309(5741):1732-1735. doi:10.1126/science.1114297

870 21. Leu JIJ, Dumont P, Hafey M, Murphy ME, George DL. Mitochondrial p53 activates Bak
871 and causes disruption of a Bak-Mcl1 complex. *Nat Cell Biol*. 2004;6(5):443-450.
872 doi:10.1038/ncb1123

873 22. Tait SWG, Parsons MJ, Llambi F, et al. Resistance to caspase-independent cell death
874 requires persistence of intact mitochondria. *Dev Cell*. 2010;18(5):802-813.
875 doi:10.1016/j.devcel.2010.03.014

876 23. Boettcher S, Miller PG, Sharma R, et al. A dominant-negative effect drives selection of
877 TP53 missense mutations in myeloid malignancies. *Science*. 2019;365(6453):599-604.
878 doi:10.1126/science.aax3649

879 24. Aubrey BJ, Kelly GL, Janic A, Herold MJ, Strasser A. How does p53 induce apoptosis
880 and how does this relate to p53-mediated tumour suppression? *Cell Death Differ*.
881 2018;25(1):104-113. doi:10.1038/cdd.2017.169

882 25. Diepstraten ST, Yuan Y, La Marca JE, et al. Putting the STING back into BH3-mimetic
883 drugs for TP53-mutant blood cancers. *Cancer Cell*. 2024;42(5):850-868.e9.
884 doi:10.1016/j.ccell.2024.04.004

885 26. Bhatt S, Pioso MS, Olesinski EA, et al. Reduced Mitochondrial Apoptotic Priming
886 Drives Resistance to BH3 Mimetics in Acute Myeloid Leukemia. *Cancer Cell*.
887 2020;38(6):872-890.e6. doi:10.1016/j.ccell.2020.10.010

888 27. Zhang Q, Riley-Gillis B, Han L, et al. Activation of RAS/MAPK pathway confers MCL-
889 1 mediated acquired resistance to BCL-2 inhibitor venetoclax in acute myeloid leukemia.
890 *Signal Transduct Target Ther*. 2022;7(1):1-13. doi:10.1038/s41392-021-00870-3

891 28. Niu X, Zhao J, Ma J, et al. Binding of Released Bim to Mcl-1 is a Mechanism of Intrinsic
892 Resistance to ABT-199 which can be Overcome by Combination with Daunorubicin or
893 Cytarabine in AML Cells. *Clin Cancer Res Off J Am Assoc Cancer Res*.
894 2016;22(17):4440-4451. doi:10.1158/1078-0432.CCR-15-3057

895 29. Ramsey HE, Fischer MA, Lee T, et al. A Novel MCL1 Inhibitor Combined with
896 Venetoclax Rescues Venetoclax-Resistant Acute Myelogenous Leukemia. *Cancer*
897 *Discov*. 2018;8(12):1566-1581. doi:10.1158/2159-8290.CD-18-0140

898 30. Carter BZ, Mak PY, Tao W, et al. Targeting MCL-1 dysregulates cell metabolism and
899 leukemia-stroma interactions and resensitizes acute myeloid leukemia to BCL-2
900 inhibition. *Haematologica*. 2022;107(1):58-76. doi:10.3324/haematol.2020.260331

901 31. Yuda J, Will C, Phillips DC, et al. Selective MCL-1 inhibitor ABBV-467 is efficacious in
902 tumor models but is associated with cardiac troponin increases in patients. *Commun Med*.
903 2023;3(1):154. doi:10.1038/s43856-023-00380-z

904 32. Amarante-Mendes GP, Finucane DM, Martin SJ, Cotter TG, Salvesen GS, Green DR.
905 Anti-apoptotic oncogenes prevent caspase-dependent and independent commitment for
906 cell death. *Cell Death Differ*. 1998;5(4):298-306. doi:10.1038/sj.cdd.4400354

907 33. McCarthy NJ, Evan GI. 15 Methods for Detecting and Quantifying Apoptosis. In: de
908 Pablo F, Ferrús A, Stern CD, eds. *Current Topics in Developmental Biology*. Vol 36.
909 Cellular and Molecular Procedures in Developmental Biology. Academic Press;
910 1997:259-278. doi:10.1016/S0070-2153(08)60507-4

911 34. Bratton SB, Salvesen GS. Regulation of the Apaf-1–caspase-9 apoptosome. *J Cell Sci*.
912 2010;123(19):3209. doi:10.1242/jcs.073643

913 35. Cepero E, King AM, Coffey LM, Perez RG, Boise LH. Caspase-9 and effector caspases
914 have sequential and distinct effects on mitochondria. *Oncogene*. 2005;24(42):6354-6366.
915 doi:10.1038/sj.onc.1208793

916 36. Ricci JE, Gottlieb RA, Green DR. Caspase-mediated loss of mitochondrial function and
917 generation of reactive oxygen species during apoptosis. *J Cell Biol*. 2003;160(1):65-75.
918 doi:10.1083/jcb.200208089

919 37. Doench JG, Fusi N, Sullender M, et al. Optimized sgRNA design to maximize activity
920 and minimize off-target effects of CRISPR-Cas9. *Nat Biotechnol*. 2016;34(2):184-191.
921 doi:10.1038/nbt.3437

922 38. Dohi T, Okada K, Xia F, et al. An IAP-IAP Complex Inhibits Apoptosis *. *J Biol Chem*.
923 2004;279(33):34087-34090. doi:10.1074/jbc.C400236200

39. Hoffman WH, Biade S, Zilfou JT, Chen J, Murphy M. Transcriptional repression of the anti-apoptotic survivin gene by wild type p53. *J Biol Chem*. 2002;277(5):3247-3257. doi:10.1074/jbc.M106643200

40. Bratton SB, Walker G, Srinivasula SM, et al. Recruitment, activation and retention of caspases-9 and -3 by Apaf-1 apoptosome and associated XIAP complexes. *EMBO J*. 2001;20(5):998. doi:10.1093/emboj/20.5.998

41. Hao Y, Sekine K, Kawabata A, et al. Apollon ubiquitinates SMAC and caspase-9, and has an essential cytoprotection function. *Nat Cell Biol*. 2004;6(9):849-860. doi:10.1038/ncb1159

42. Carter BZ, Qiu Y, Huang X, et al. Survivin is highly expressed in CD34+38− leukemic stem/progenitor cells and predicts poor clinical outcomes in AML. *Blood*. 2012;120(1):173-180. doi:10.1182/blood-2012-02-409888

43. Carter BZ, Wang RY, Schober WD, Milella M, Chism D, Andreeff M. Targeting Survivin expression induces cell proliferation defect and subsequent cell death involving mitochondrial pathway in myeloid leukemic cells. *Cell Cycle Georget Tex*. 2003;2(5):488-493.

44. Ventura A, Kirsch DG, McLaughlin ME, et al. Restoration of p53 function leads to tumour regression in vivo. *Nature*. 2007;445(7128):661-665. doi:10.1038/nature05541

45. Gholizadeh S, Dolman EM, Wieriks R, Sparidans RW, Hennink WE, Kok RJ. Anti-GD2 Immunoliposomes for Targeted Delivery of the Survivin Inhibitor Sepantronium Bromide (YM155) to Neuroblastoma Tumor Cells. *Pharm Res*. 2018;35(4):85. doi:10.1007/s11095-018-2373-x

46. Chen X, Glytsou C, Zhou H, et al. Targeting Mitochondrial Structure Sensitizes Acute Myeloid Leukemia to Venetoclax Treatment. *Cancer Discov*. 2019;9(7):890-909. doi:10.1158/2159-8290.CD-19-0117

47. Nechiporuk T, Kurtz SE, Nikolova O, et al. The TP53 Apoptotic Network Is a Primary Mediator of Resistance to BCL2 Inhibition in AML Cells. *Cancer Discov*. 2019;9(7):910-925. doi:10.1158/2159-8290.CD-19-0125

48. Savona MR, Rathmell JC. Mitochondrial Homeostasis in AML and Gasping for Response in Resistance to BCL2 Blockade. *Cancer Discov*. 2019;9(7):831-833. doi:10.1158/2159-8290.CD-19-0510

49. Sallman DA, DeZern AE, Garcia-Manero G, et al. Eprenetapopt (APR-246) and Azacitidine in TP53-Mutant Myelodysplastic Syndromes. *J Clin Oncol Off J Am Soc Clin Oncol*. 2021;39(14):1584-1594. doi:10.1200/JCO.20.02341

50. McKinnell Z, Karel D, Tuerff D, Abrahim MS, Nassereddine S. Acute Myeloid Leukemia Following Myeloproliferative Neoplasms: A Review of What We Know, What We Do Not Know, and Emerging Treatment Strategies. *J Hematol*. 2023;11(6):197-209.

51. Lawrence L. Magrolimab/Azacitidine Combo Shows Efficacy for Untreated TP53-Mutant AML. Published online November 30, 2023. Accessed July 13,

963 2024. https://ashpublications.org/ashclinicalnews/news/7523/Magrolimab-Azacitidine-
964 Combo-Shows-Efficacy-for

965 52. Sallman DA, Al Malki MM, Asch AS, et al. Magrolimab in Combination With
966 Azacitidine in Patients With Higher-Risk Myelodysplastic Syndromes: Final Results of a
967 Phase Ib Study. *J Clin Oncol*. 2023;41(15):2815-2826. doi:10.1200/JCO.22.01794

968 53. Thijssen R, Diepstraten ST, Moujalled D, et al. Intact TP-53 function is essential for
969 sustaining durable responses to BH3-mimetic drugs in leukemias. *Blood*.
970 2021;137(20):2721-2735. doi:10.1182/blood.2020010167

971 54. Nishida Y, Ishizawa J, Ayoub E, et al. Enhanced TP53 reactivation disrupts MYC
972 transcriptional program and overcomes venetoclax resistance in acute myeloid leukemias.
973 *Sci Adv*. 2023;9(48):eadh1436. doi:10.1126/sciadv.adh1436

974 55. Hassin O, Nataraj NB, Shreberk-Shaked M, et al. Different hotspot p53 mutants exert
975 distinct phenotypes and predict outcome of colorectal cancer patients. *Nat Commun*.
976 2022;13(1):2800. doi:10.1038/s41467-022-30481-7

977 56. Mirza A, McGuirk M, Hockenberry TN, et al. Human survivin is negatively regulated by
978 wild-type p53 and participates in p53-dependent apoptotic pathway. *Oncogene*.
979 2002;21(17):2613-2622. doi:10.1038/sj.onc.1205353

980 57. Jaiswal PK, Goel A, Mittal RD. Survivin: A molecular biomarker in cancer. *Indian J Med*
981 *Res*. 2015;141(4):389-397. doi:10.4103/0971-5916.159250

982 58. Velculescu VE, Madden SL, Zhang L, et al. Analysis of human transcriptomes. *Nat*
983 *Genet*. 1999;23(4):387-388. doi:10.1038/70487

984 59. Marusawa H, Matsuzawa S, Welsh K, et al. HBXIP functions as a cofactor of survivin in
985 apoptosis suppression. *EMBO J*. 2003;22(11):2729-2740. doi:10.1093/emboj/cdg263

986 60. Rongvaux A, Willinger T, Martinek J, et al. Development and function of human innate
987 immune cells in a humanized mouse model. *Nat Biotechnol*. 2014;32(4):364-372.
988 doi:10.1038/nbt.2858

989 61. Ryan J, Montero J, Rocco J, Letai A. iBH3: simple, fixable BH3 profiling to determine
990 apoptotic priming in primary tissue by flow cytometry. *Biol Chem*. 2016;397(7):671-678.
991 doi:10.1515/hsz-2016-0107

992 62. Miller PG, Sperling AS, Mayerhofer C, et al. PPM1D modulates hematopoietic cell
993 fitness and response to DNA damage and is a therapeutic target in myeloid malignancy.
994 *Blood*. 2023;142(24):2079-2091. doi:10.1182/blood.2023020331

995 63. Li W, Xu H, Xiao T, et al. MAGeCK enables robust identification of essential genes from
996 genome-scale CRISPR/Cas9 knockout screens. *Genome Biol*. 2014;15(12):554.
997 doi:10.1186/s13059-014-0554-4

998 64. Li W, Köster J, Xu H, et al. Quality control, modeling, and visualization of CRISPR
999 screens with MAGeCK-VISPR. *Genome Biol*. 2015;16:281. doi:10.1186/s13059-015-
1000 0843-6

1001 65. Wang B, Wang M, Zhang W, et al. Integrative analysis of pooled CRISPR genetic
1002 screens using MAGeCKFlute. *Nat Protoc*. 2019;14(3):756-780. doi:10.1038/s41596-018-
1003 0113-7

1004 66. Steinebach C, Bricelj A, Murgai A, et al. Leveraging Ligand Affinity and Properties:
1005 Discovery of Novel Benzamide-Type Cereblon Binders for the Design of PROTACs. *J*
1006 *Med Chem*. 2023;66(21):14513-14543. doi:10.1021/acs.jmedchem.3c00851

1007 67. Demichev V, Messner CB, Vernardis SI, Lilley KS, Ralser M. DIA-NN: neural networks
1008 and interference correction enable deep proteome coverage in high throughput. *Nat*
1009 *Methods*. 2020;17(1):41-44. doi:10.1038/s41592-019-0638-x

1010 68. Ritchie ME, Phipson B, Wu D, et al. limma powers differential expression analyses for
1011 RNA-sequencing and microarray studies. *Nucleic Acids Res*. 2015;43(7):e47.
1012 doi:10.1093/nar/gkv007

1013 69. Tyner JW, Tognon CE, Bottomly D, et al. Functional genomic landscape of acute
1014 myeloid leukaemia. *Nature*. 2018;562(7728):526-531. doi:10.1038/s41586-018-0623-z

1015 70. de Camargo Magalhães ES, Hubner SE, Brown BD, Qiu Y, Kornblau SM. Proteomics for
1016 optimizing therapy in acute myeloid leukemia: venetoclax plus hypomethylating agents
1017 versus conventional chemotherapy. *Leukemia*. 2024;38(5):1046-1056.
1018 doi:10.1038/s41375-024-02208-8

1019 71. Hoff FW, Hu CW, Qiu Y, et al. Recognition of Recurrent Protein Expression Patterns in
1020 Pediatric Acute Myeloid Leukemia Identified New Therapeutic Targets. *Mol Cancer Res*
1021 *MCR*. 2018;16(8):1275-1286. doi:10.1158/1541-7786.MCR-17-0731

1022 72. van Dijk AD, Hoff FW, Qiu YH, et al. Loss of H3K27 methylation identifies poor
1023 outcomes in adult-onset acute leukemia. *Clin Epigenetics*. 2021;13(1):21.
1024 doi:10.1186/s13148-021-01011-x

1025 73. Griffen TL, Hoff FW, Qiu Y, et al. Proteomic profiling based classification of CLL
1026 provides prognostication for modern therapy and identifies novel therapeutic targets.
1027 *Blood Cancer J*. 2022;12(3):43. doi:10.1038/s41408-022-00623-7

1028 74. Kornblau SM, Coombes KR. Use of reverse phase protein microarrays to study protein
1029 expression in leukemia: technical and methodological lessons learned. *Methods Mol Biol*
1030 *Clifton NJ*. 2011;785:141-155. doi:10.1007/978-1-61779-286-1_10

1031 75. Kornblau SM, Womble M, Qiu YH, et al. Simultaneous activation of multiple signal
1032 transduction pathways confers poor prognosis in acute myelogenous leukemia. *Blood*.
1033 2006;108(7):2358-2365. doi:10.1182/blood-2006-02-003475

1034 76. Carter BZ, Mak PY, Tao W, et al. Combined inhibition of BCL-2 and MCL-1 overcomes
1035 BAX deficiency-mediated resistance of TP53-mutant acute myeloid leukemia to
1036 individual BH3 mimetics. *Blood Cancer J*. 2023;13(1):1-13. doi:10.1038/s41408-023-
1037 00830-w

1038 77. Dobin A, Davis CA, Schlesinger F, et al. STAR: ultrafast universal RNA-seq aligner.
1039 *Bioinforma Oxf Engl*. 2013;29(1):15-21. doi:10.1093/bioinformatics/bts635

1040 78. Love MI, Huber W, Anders S. Moderated estimation of fold change and dispersion for
1041 RNA-seq data with DESeq2. *Genome Biol*. 2014;15(12):550. doi:10.1186/s13059-014-
1042 0550-8

1043 79. Gao T, Soldatov R, Sarkar H, et al. Haplotype-aware analysis of somatic copy number
1044 variations from single-cell transcriptomes. *Nat Biotechnol*. 2023;41(3):417-426.
1045 doi:10.1038/s41587-022-01468-y

1046 80. Wolf FA, Angerer P, Theis FJ. SCANPY: large-scale single-cell gene expression data
1047 analysis. *Genome Biol*. 2018;19(1):15. doi:10.1186/s13059-017-1382-0

1048 81. Domínguez Conde C, Xu C, Jarvis LB, et al. Cross-tissue immune cell analysis reveals
1049 tissue-specific features in humans. *Science*. 2022;376(6594):eabl5197.
1050 doi:10.1126/science.abl5197

1051

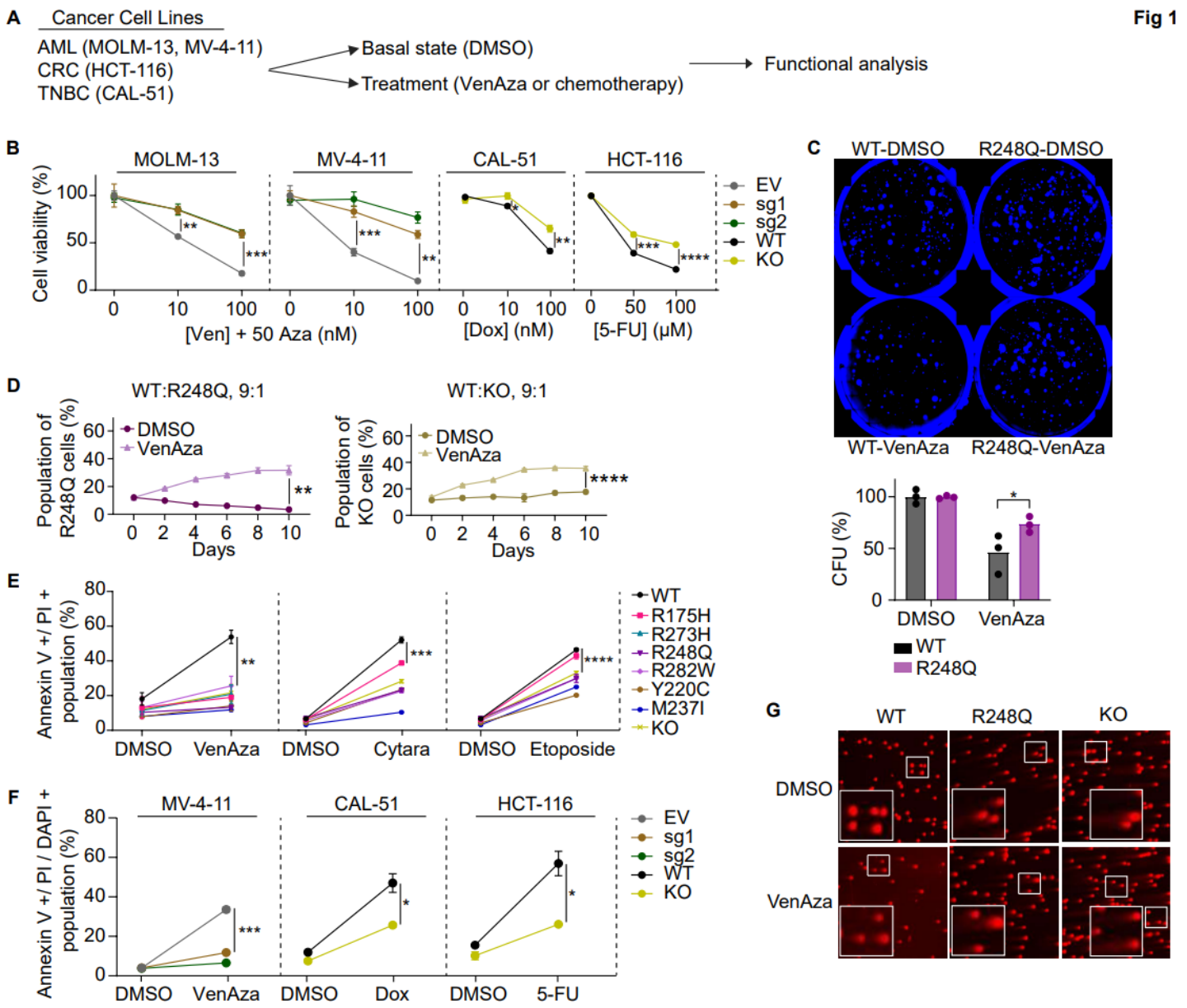
A
Cancer Cell Lines
AML (MOLM-13, MV-4-11)
CRC (HCT-116)
TNBC (CAL-51)
Basal state (DMSO)
Treatment (VenAza or chemotherapy)
Functional analysis
B
MOLM-13
MV-4-11
CAL-51
HCT-116
Cell viability (%)
[Ven] + 50 Aza (nM)
[Dox] (nM)
[5-FU] (μM)
EV
sg1
sg2
WT
KO
C
WT-DMSO
R248Q-DMSO
WT-VenAza
R248Q-VenAza
CFU (%)
DMSO
VenAza
WT
R248Q
D
WT:R248Q, 9:1
WT:KO, 9:1
Population of R248Q cells (%)
Population of KO cells (%)
Days
DMSO
VenAza
E
Annexin V +/ PI + population (%)
DMSO
VenAza
Cytara
Etoposide
WT
R175H
R273H
R248Q
R282W
Y220C
M237I
KO
F
MV-4-11
CAL-51
HCT-116
Annexin V +/ PI / DAPI + population (%)
DMSO
VenAza
Dox
5-FU
EV
sg1
sg2
WT
KO
G
WT
R248Q
KO
DMSO
VenAza

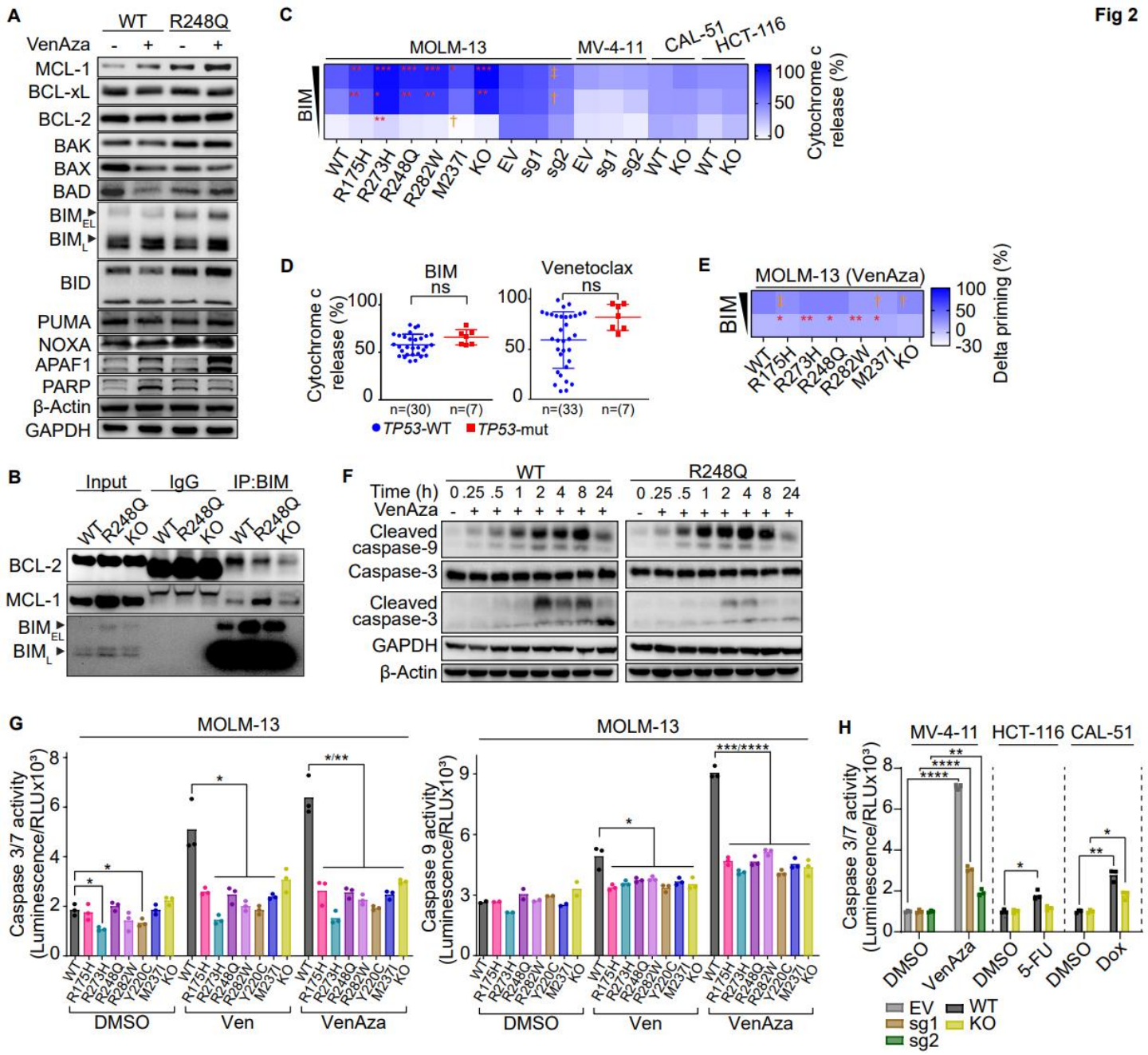
A
WT
R248Q
VenAza
MCL-1
BCL-xL
BCL-2
BAK
BAX
BAD
BIM EL
BIM L
BID
PUMA
NOXA
APAF1
PARP
β-Actin
GAPDH
B
Input
IgG
IP:BIM
WT
R248Q
KO
BCL-2
MCL-1
BIM EL
BIM L
C
MOLM-13
MV-4-11
CAL-51
HCT-116
BIM
Cytochrome c release (%)
WT
R175H
R273H
R248Q
R282W
M237I
KO
EV
sg1
sg2
D
BIM
Venetoclax
ns
Cytochrome c release (%)
n=(30)
n=(7)
n=(33)
TP53-WT
TP53-mut
E
MOLM-13 (VenAza)
BIM
Delta priming (%)
F
WT
R248Q
Time (h)
VenAza
Cleaved caspase-9
Caspase-3
Cleaved caspase-3
GAPDH
β-Actin
G
MOLM-13
Caspase 3/7 activity (Luminescence/RLUx10³)
Caspase 9 activity (Luminescence/RLUx10³)
Y220C
DMSO
Ven
VenAza
H
MV-4-11
HCT-116
CAL-51
Caspase 3/7 activity (Luminescence/RLUx10³)
DMSO
VenAza
5-FU
Dox
EV
sg1
sg2
WT
KO

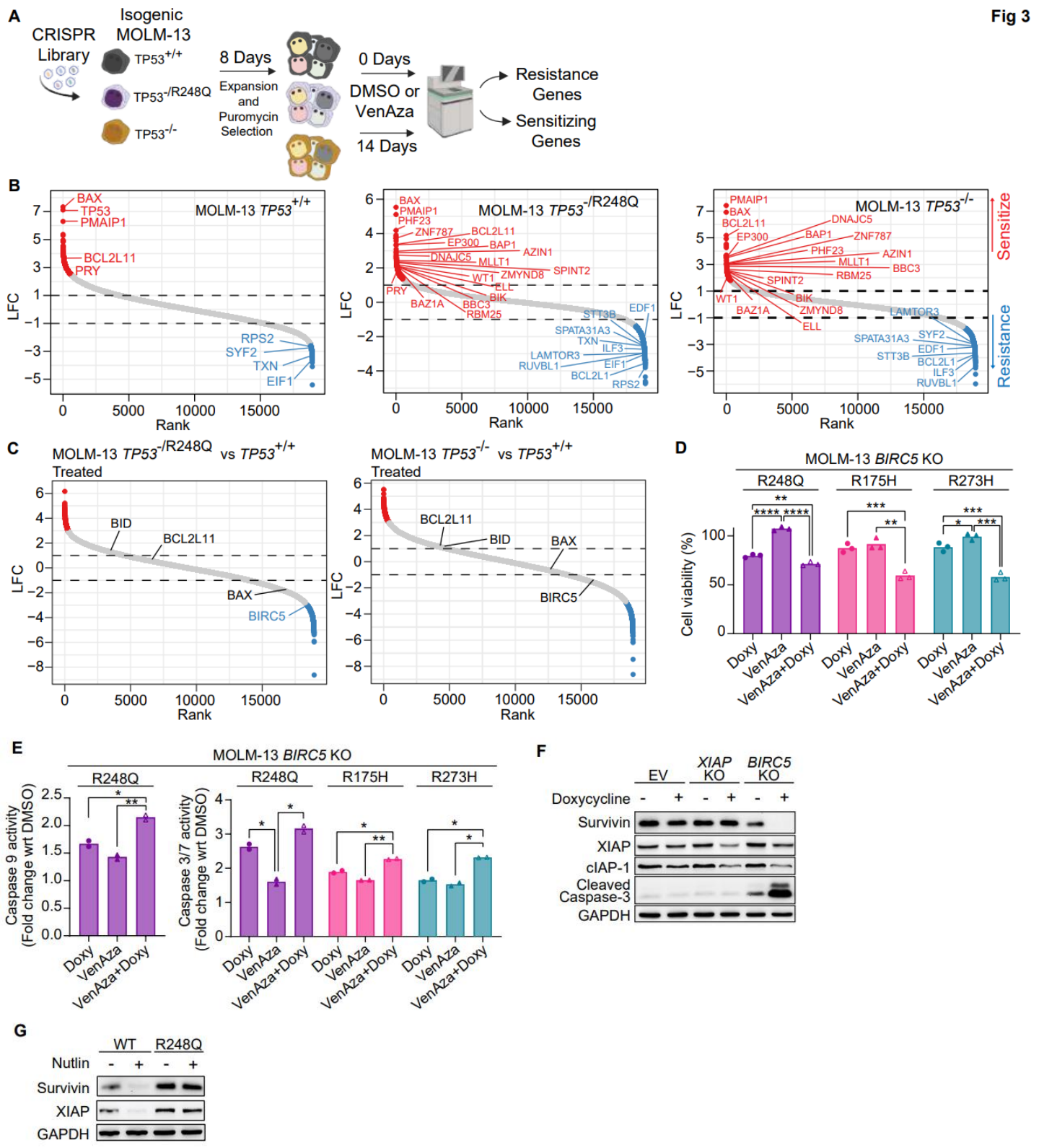
A
CRISPR Library
Isogenic MOLM-13
TP53+/+
TP53-/R248Q
TP53-/-
8 Days
Expansion and Puromycin Selection
0 Days
DMSO or VenAza
14 Days
Resistance Genes
Sensitizing Genes
B
MOLM-13 TP53+/+
MOLM-13 TP53-/R248Q
MOLM-13 TP53-/-
Sensitize
Resistance
LFC
Rank
C
MOLM-13 TP53-/R248Q vs TP53+/+
Treated
MOLM-13 TP53-/- vs TP53+/+
Treated
D
MOLM-13 BIRC5 KO
R248Q
R175H
R273H
Cell viability (%)
Doxy
VenAza
VenAza+Doxy
E
MOLM-13 BIRC5 KO
Caspase 9 activity (Fold change wrt DMSO)
Caspase 3/7 activity (Fold change wrt DMSO)
F
EV
XIAP KO
BIRC5 KO
Doxycycline
Survivin
XIAP
cIAP-1
Cleaved Caspase-3
GAPDH
G
WT
R248Q
Nutlin
Survivin
XIAP
GAPDH

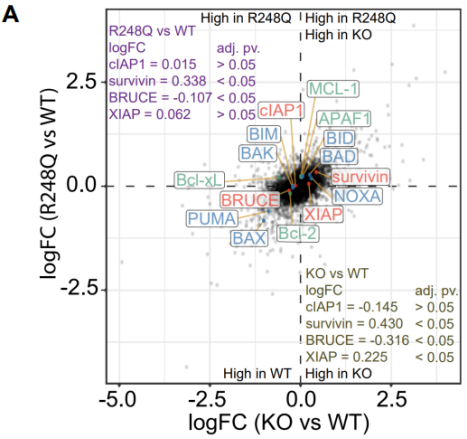
A
High in R248Q
High in R248Q
High in KO
R248Q vs WT
logFC
adj. pv.
cIAP1 = 0.015 > 0.05
survivin = 0.338 < 0.05
BRUCE = -0.107 < 0.05
XIAP = 0.062 > 0.05
MCL-1
cIAP1
APAF1
BIM
BID
BAK
BAD
Bcl-xL
survivin
BRUCE
NOXA
PUMA
XIAP
BAX
Bcl-2
KO vs WT
logFC
adj. pv.
cIAP1 = -0.145 > 0.05
survivin = 0.430 < 0.05
BRUCE = -0.316 < 0.05
XIAP = 0.225 < 0.05
High in WT
High in KO
logFC (R248Q vs WT)
logFC (KO vs WT)

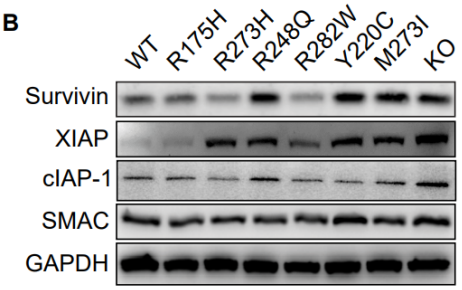
B
WT
R175H
R273H
R248Q
R282W
Y220C
M273I
KO
Survivin
XIAP
cIAP-1
SMAC
GAPDH

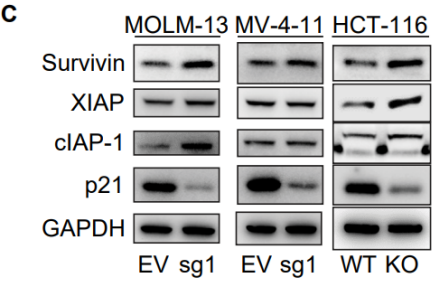
C
MOLM-13
MV-4-11
HCT-116
Survivin
XIAP
cIAP-1
p21
GAPDH
EV
sg1
EV
sg1
WT
KO

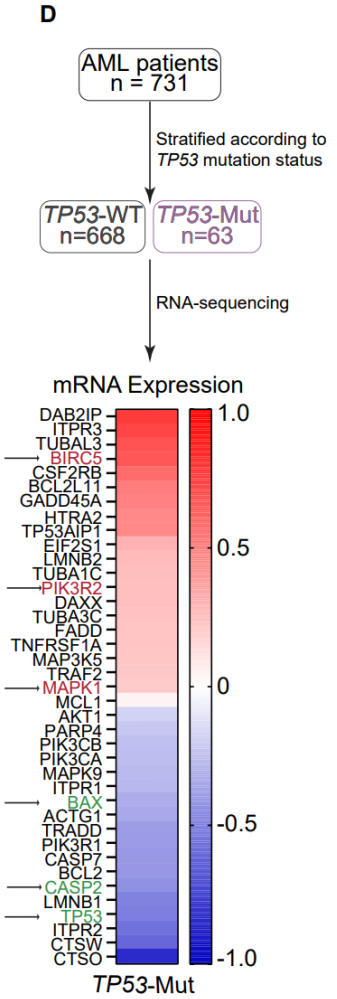
D
AML patients
n = 731
Stratified according to
TP53 mutation status
TP53-WT
n=668
TP53-Mut
n=63
RNA-sequencing
mRNA Expression
DAB2IP
ITPR3
TUBAL3
BIRC5
CSF2RB
BCL2L11
GADD45A
HTRA2
TP53AIP1
EIF2S1
LMNB2
TUBA1C
PIK3R2
DAXX
TUBA3C
FADD
TNFRSF1A
MAP3K5
TRAF2
MAPK1
MCL1
AKT1
PARP4
PIK3CB
PIK3CA
MAPK9
ITPR1
BAX
ACTG1
TRADD
PIK3R1
CASP7
BCL2
CASP2
LMNB1
TP53
ITPR2
CTSW
CTSO
1.0
0.5
0
-0.5
-1.0
TP53-Mut

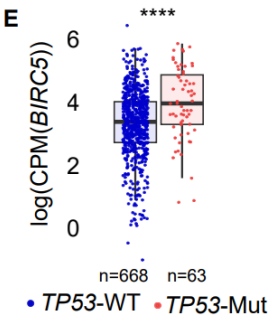
E
****
log(CPM(BIRC5))
6
4
2
0
n=668
n=63
TP53-WT
TP53-Mut

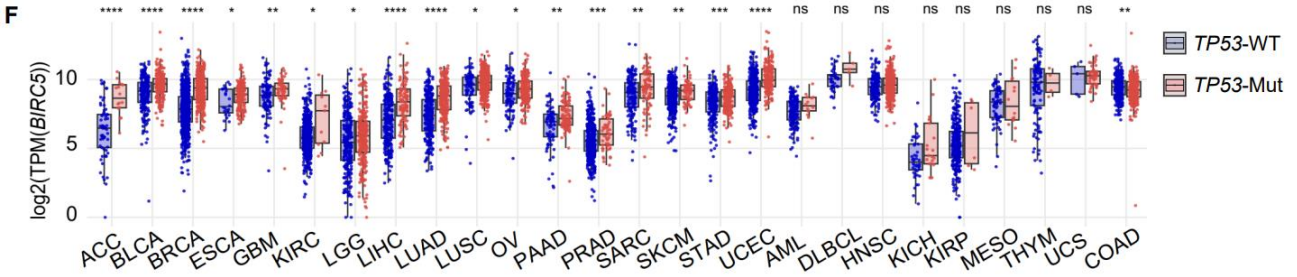
F
log2(TPM(BIRC5))
10
5
0
ACC
BLCA
BRCA
ESCA
GBM
KIRC
LGG
LIHC
LUAD
LUSC
OV
PAAD
PRAD
SARC
SKCM
STAD
UCEC
AML
DLBCL
HNSC
KICH
KIRP
MESO
THYM
UCS
COAD
TP53-WT
TP53-Mut

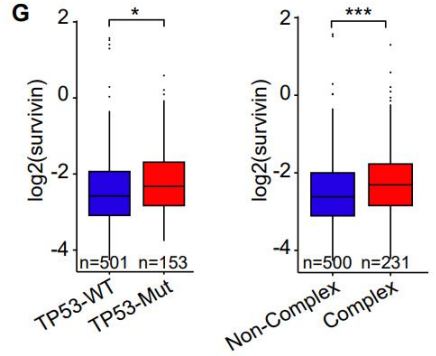
G
log2(survivin)
*
n=501
n=153
TP53-WT
TP53-Mut
***
n=500
n=231
Non-Complex
Complex

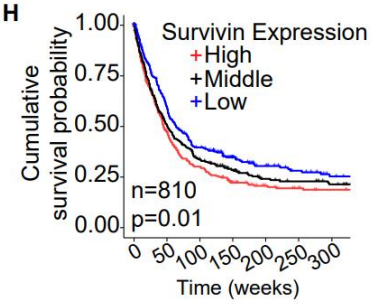
H
Survivin Expression
High
Middle
Low
Cumulative survival probability
1.00
0.75
0.50
0.25
0.00
n=810
p=0.01
0
50
100
150
200
250
300
Time (weeks)

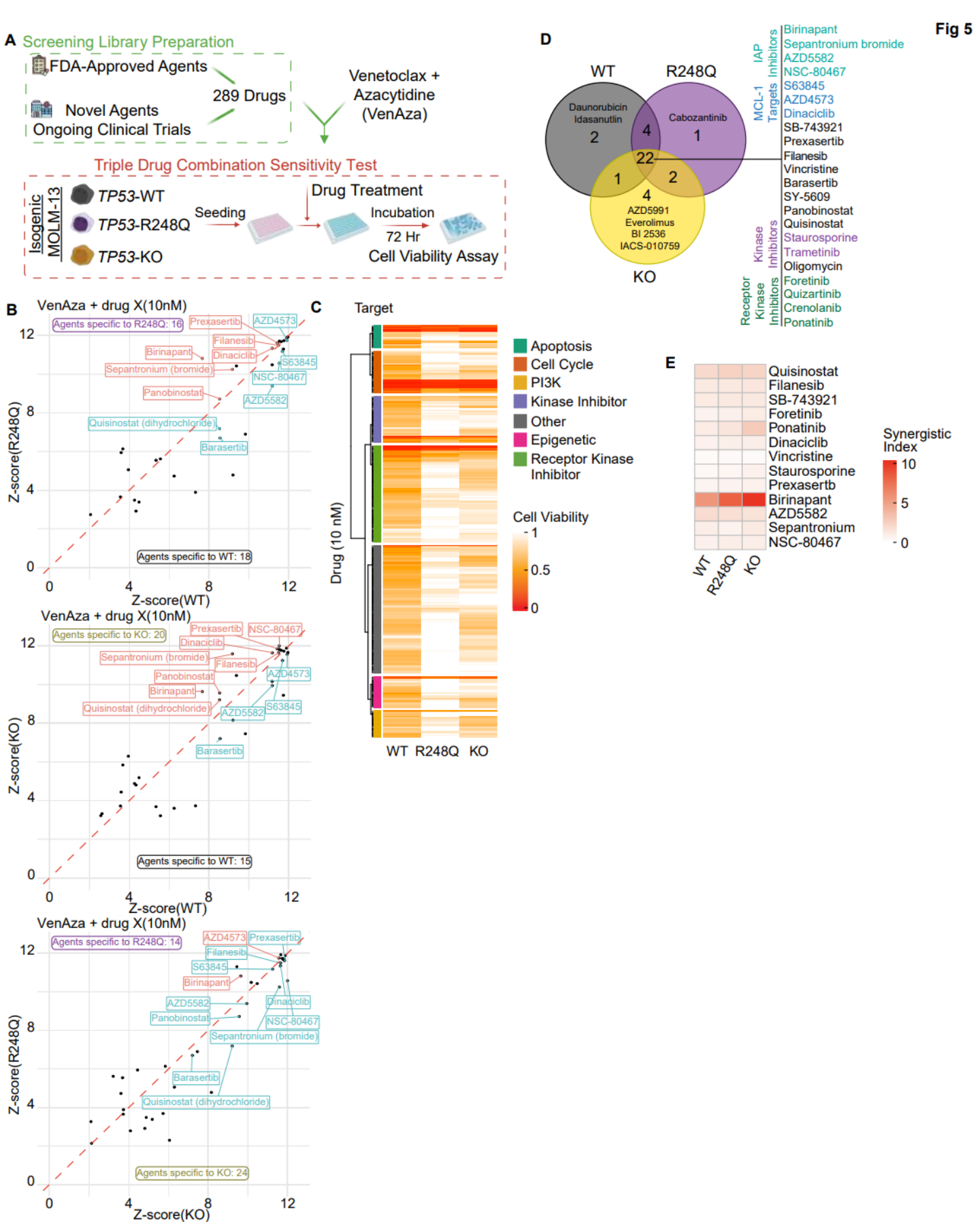
Fig 5
A
Screening Library Preparation
FDA-Approved Agents
Novel Agents
Ongoing Clinical Trials
289 Drugs
Venetoclax + Azacytidine (VenAza)
Triple Drug Combination Sensitivity Test
Isogenic MOLM-13
TP53-WT
TP53-R248Q
TP53-KO
Seeding
Drug Treatment
Incubation
72 Hr
Cell Viability Assay
B
VenAza + drug X(10nM)
Agents specific to R248Q: 16
Agents specific to WT: 18
Z-score(R248Q)
Z-score(WT)
Agents specific to KO: 20
Agents specific to WT: 15
Z-score(KO)
Agents specific to R248Q: 14
Agents specific to KO: 24
C
Target
Drug (10 nM)
Apoptosis
Cell Cycle
PI3K
Kinase Inhibitor
Other
Epigenetic
Receptor Kinase Inhibitor
Cell Viability
WT R248Q KO
D
WT
R248Q
KO
Daunorubicin
Idasanutlin
Cabozantinib
AZD5991
Everolimus
BI 2536
IACS-010759
IAP Inhibitors
MCL-1 Targets
Kinase Inhibitors
Receptor Kinase Inhibitors
Birinapant
Sepantronium bromide
AZD5582
NSC-80467
S63845
AZD4573
Dinaciclib
SB-743921
Prexasertib
Filanesib
Vincristine
Barasertib
SY-5609
Panobinostat
Quisinostat
Staurosporine
Trametinib
Oligomycin
Foretinib
Quizartinib
Crenolanib
Ponatinib
E
Synergistic Index

Fig 6

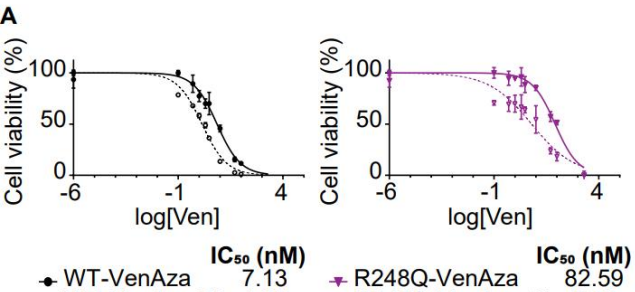
A
Cell viability (%)
log[Ven]
IC50 (nM)
WT-VenAza 7.13
WT-VenAza-Bir 1.37
R248Q-VenAza 82.59
R248Q-VenAza-Bir 6.22

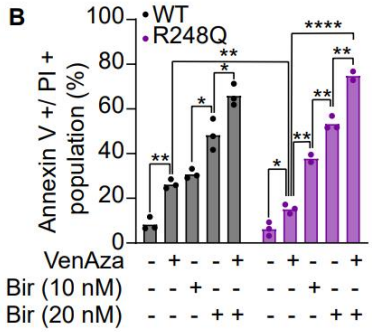
B
WT
R248Q
Annexin V +/ PI + population (%)
VenAza
Bir (10 nM)
Bir (20 nM)

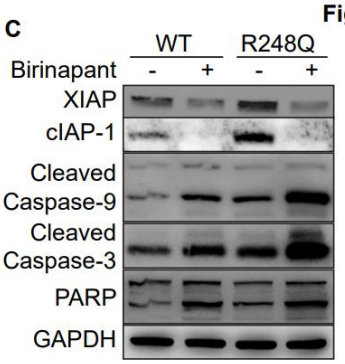
C
WT
R248Q
Birinapant
XIAP
cIAP-1
Cleaved Caspase-9
Cleaved Caspase-3
PARP
GAPDH

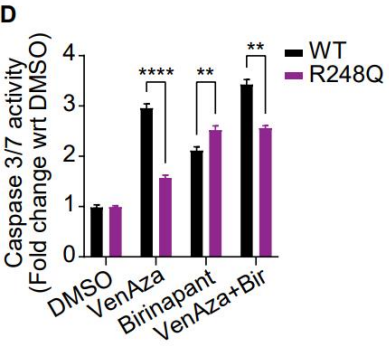
D
Caspase 3/7 activity (Fold change wrt DMSO)
WT
R248Q
DMSO
VenAza
Birinapant
VenAza+Bir

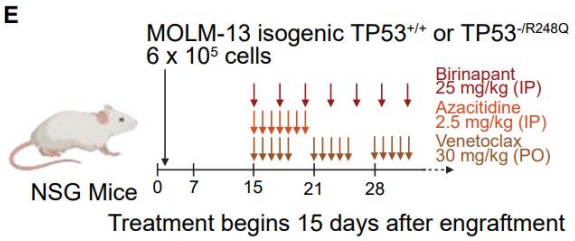
E
MOLM-13 isogenic TP53+/+ or TP53-/R248Q
6 x 10^5 cells
Birinapant 25 mg/kg (IP)
Azacitidine 2.5 mg/kg (IP)
Venetoclax 30 mg/kg (PO)
NSG Mice
0 7 15 21 28
Treatment begins 15 days after engraftment

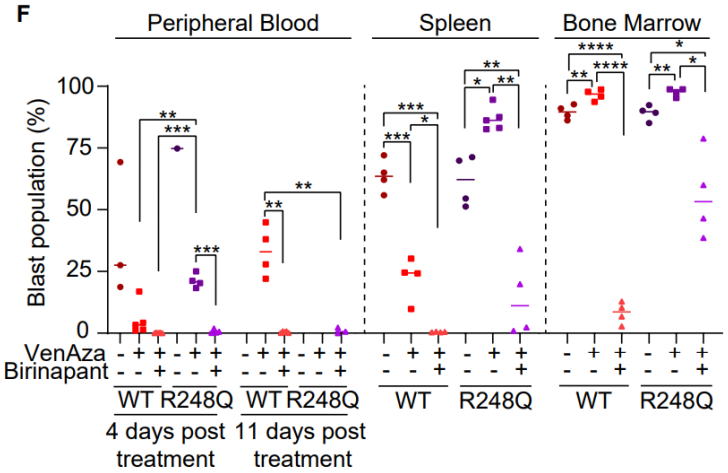
F
Peripheral Blood
Spleen
Bone Marrow
Blast population (%)
VenAza
Birinapant
WT R248Q
4 days post treatment
11 days post treatment
WT
R248Q

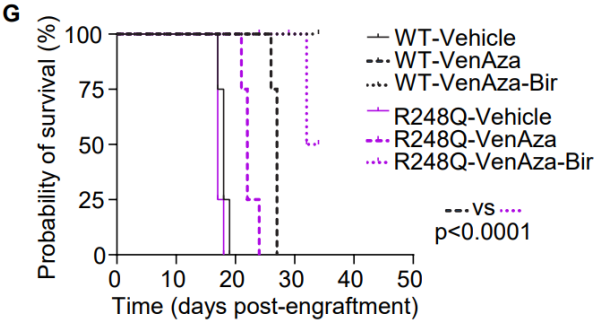
G
Probability of survival (%)
Time (days post-engraftment)
WT-Vehicle
WT-VenAza
WT-VenAza-Bir
R248Q-Vehicle
R248Q-VenAza
R248Q-VenAza-Bir
vs
p<0.0001

Fig 7

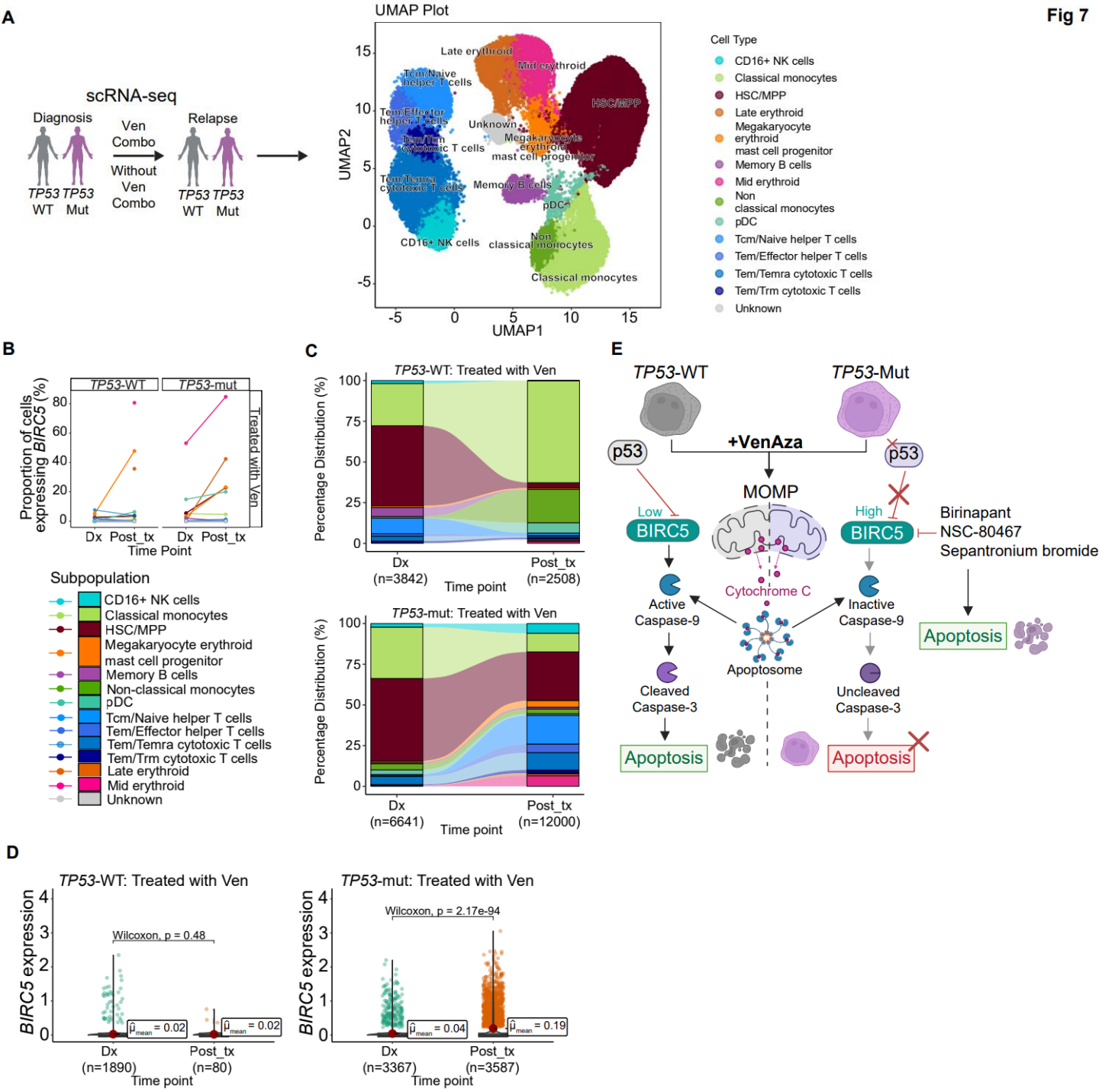
A
scRNA-seq
Diagnosis
TP53 WT
TP53 Mut
Ven Combo
Without Ven Combo
Relapse
TP53 WT
TP53 Mut
UMAP Plot
UMAP1
UMAP2
Late erythroid
Mid erythroid
HSC/MPP
Tcm/Naive helper T cells
Tem/Effector helper T cells
Unknown
Megakaryocyte erythroid mast cell progenitor
Tem/Trm cytotoxic T cells
Tem/Temra cytotoxic T cells
Memory B cells
pDC
CD16+ NK cells
Non classical monocytes
Classical monocytes
Cell Type
CD16+ NK cells
Classical monocytes
HSC/MPP
Late erythroid
Megakaryocyte erythroid mast cell progenitor
Memory B cells
Mid erythroid
Non classical monocytes
pDC
Tcm/Naive helper T cells
Tem/Effector helper T cells
Tem/Temra cytotoxic T cells
Tem/Trm cytotoxic T cells
Unknown
B
Proportion of cells expressing BIRC5 (%)
TP53-WT
TP53-mut
Treated with Ven
Dx
Post_tx
Time Point
Subpopulation
CD16+ NK cells
Classical monocytes
HSC/MPP
Megakaryocyte erythroid mast cell progenitor
Memory B cells
Non-classical monocytes
pDC
Tcm/Naive helper T cells
Tem/Effector helper T cells
Tem/Temra cytotoxic T cells
Tem/Trm cytotoxic T cells
Late erythroid
Mid erythroid
Unknown
C
TP53-WT: Treated with Ven
Percentage Distribution (%)
Dx (n=3842)
Post_tx (n=2508)
Time point
TP53-mut: Treated with Ven
Dx (n=6641)
Post_tx (n=12000)
D
TP53-WT: Treated with Ven
BIRC5 expression
Wilcoxon, p = 0.48
Dx (n=1890)
Post_tx (n=80)
Time point
TP53-mut: Treated with Ven
Wilcoxon, p = 2.17e-94
Dx (n=3367)
Post_tx (n=3587)
E
TP53-WT
TP53-Mut
+VenAza
p53
MOMP
Low
BIRC5
High
BIRC5
Birinapant
NSC-80467
Sepantronium bromide
Cytochrome C
Active Caspase-9
Inactive Caspase-9
Apoptosome
Cleaved Caspase-3
Uncleaved Caspase-3
Apoptosis

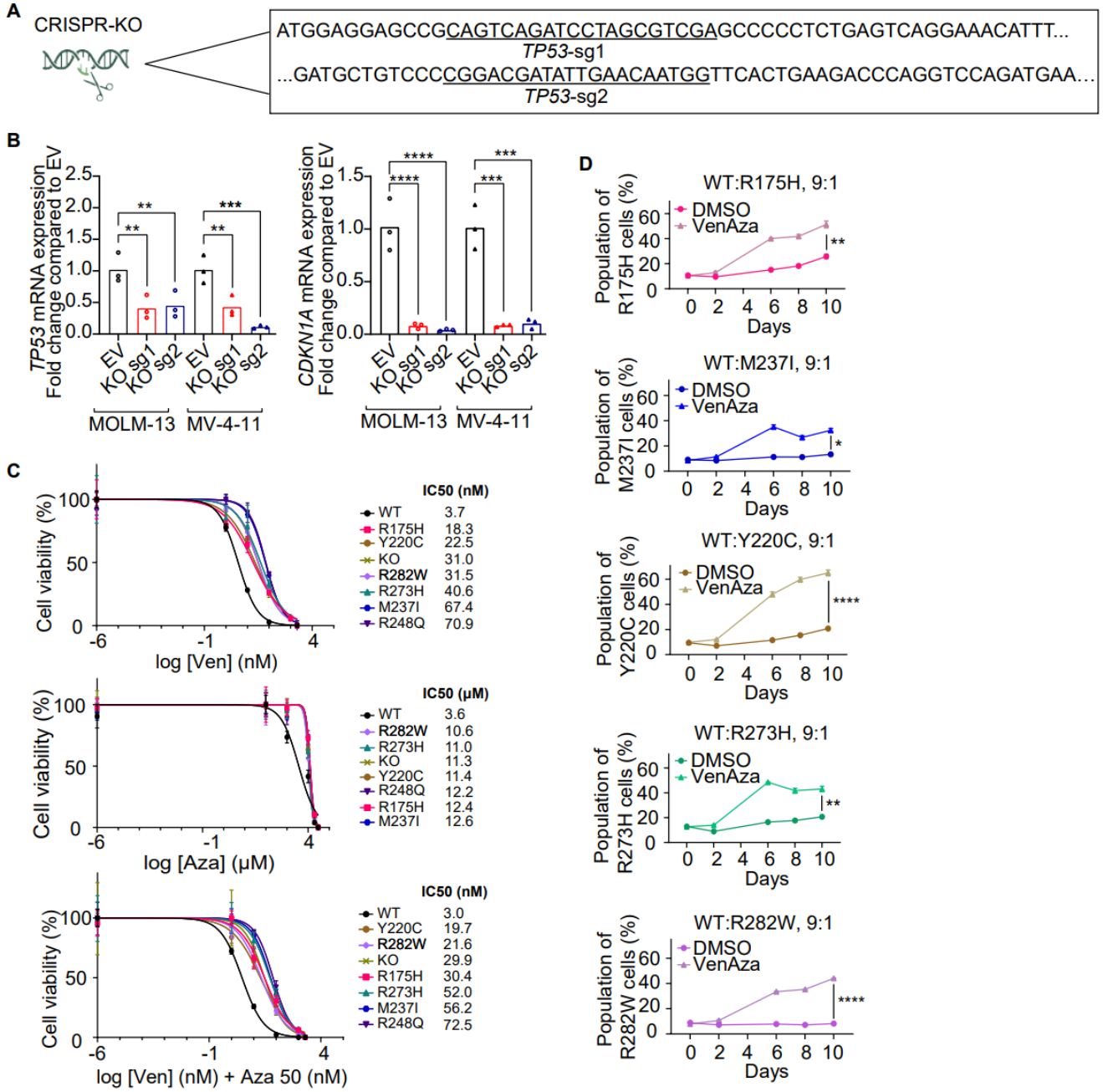
A
CRISPR-KO
ATGGAGGAGCCGCAGTCAGATCCTAGCGTCGAGCCCCCTCTGAGTCAGGAAACATTT...
TP53-sg1
...GATGCTGTCCCCGGACGATATTGAACAATGGTTCACTGAAGACCCAGGTCCAGATGAA...
TP53-sg2
B
TP53 mRNA expression Fold change compared to EV
CDKN1A mRNA expression Fold change compared to EV
EV
KO
KO sg1
KO sg2
MOLM-13
MV-4-11
C
Cell viability (%)
log [Ven] (nM)
IC50 (nM)
WT 3.7
R175H 18.3
Y220C 22.5
KO 31.0
R282W 31.5
R273H 40.6
M237I 67.4
R248Q 70.9
log [Aza] (μM)
IC50 (μM)
WT 3.6
R282W 10.6
R273H 11.0
KO 11.3
Y220C 11.4
R248Q 12.2
R175H 12.4
M237I 12.6
log [Ven] (nM) + Aza 50 (nM)
IC50 (nM)
WT 3.0
Y220C 19.7
R282W 21.6
KO 29.9
R175H 30.4
R273H 52.0
M237I 56.2
R248Q 72.5
D
WT:R175H, 9:1
WT:M237I, 9:1
WT:Y220C, 9:1
WT:R273H, 9:1
WT:R282W, 9:1
DMSO
VenAza
Population of R175H cells (%)
Population of M237I cells (%)
Population of Y220C cells (%)
Population of R273H cells (%)
Population of R282W cells (%)
Days

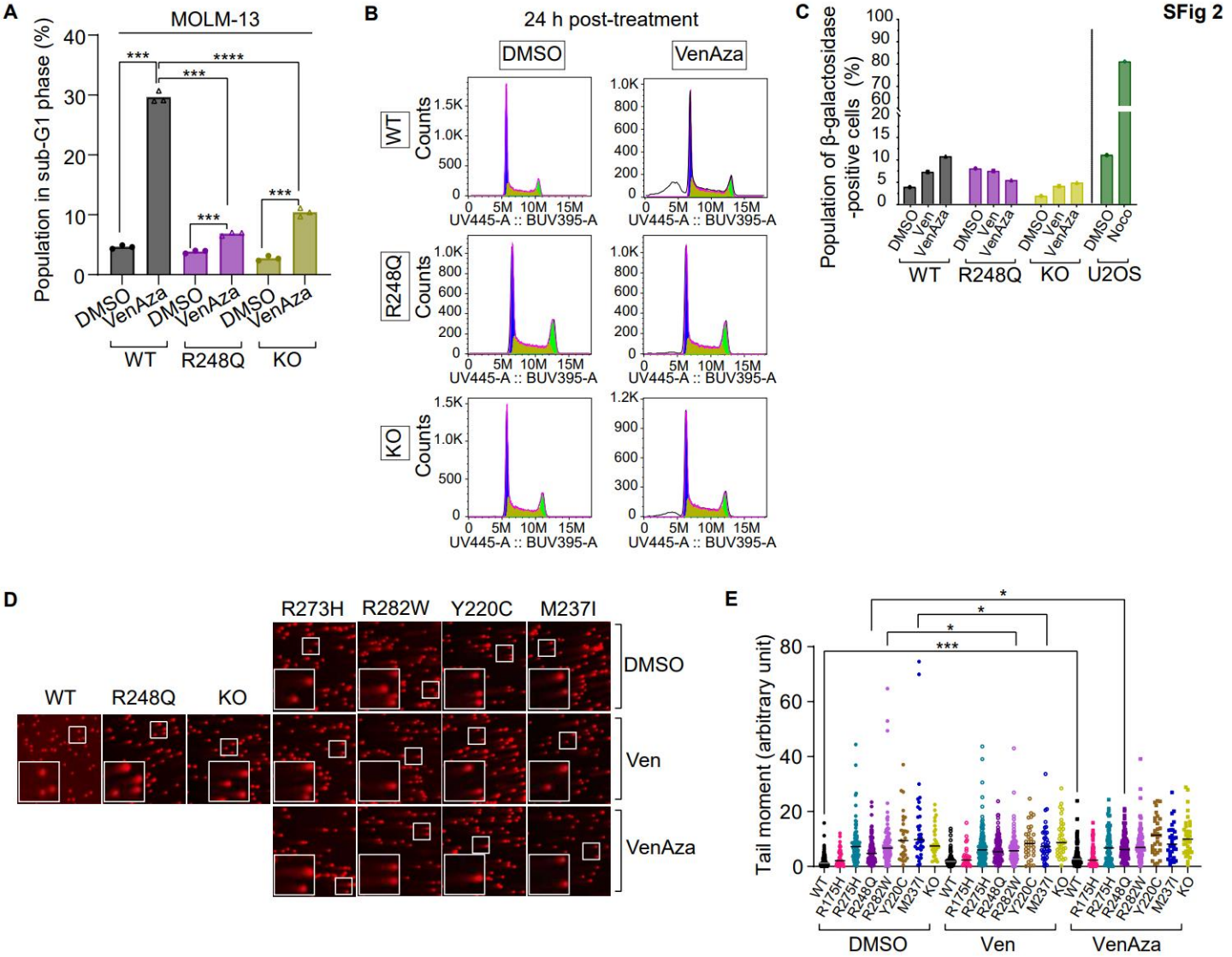
SFig 2
A
MOLM-13
Population in sub-G1 phase (%)
DMSO
VenAza
WT
R248Q
KO
B
24 h post-treatment
DMSO
VenAza
WT
R248Q
KO
Counts
UV445-A :: BUV395-A
C
Population of β-galactosidase -positive cells (%)
DMSO
Ven
VenAza
Noco
WT
R248Q
KO
U2OS
D
WT
R248Q
KO
R273H
R282W
Y220C
M237I
DMSO
Ven
VenAza
E
Tail moment (arbitrary unit)
WT
R175H
R275H
R248Q
R282W
Y220C
M237I
KO
DMSO
Ven
VenAza

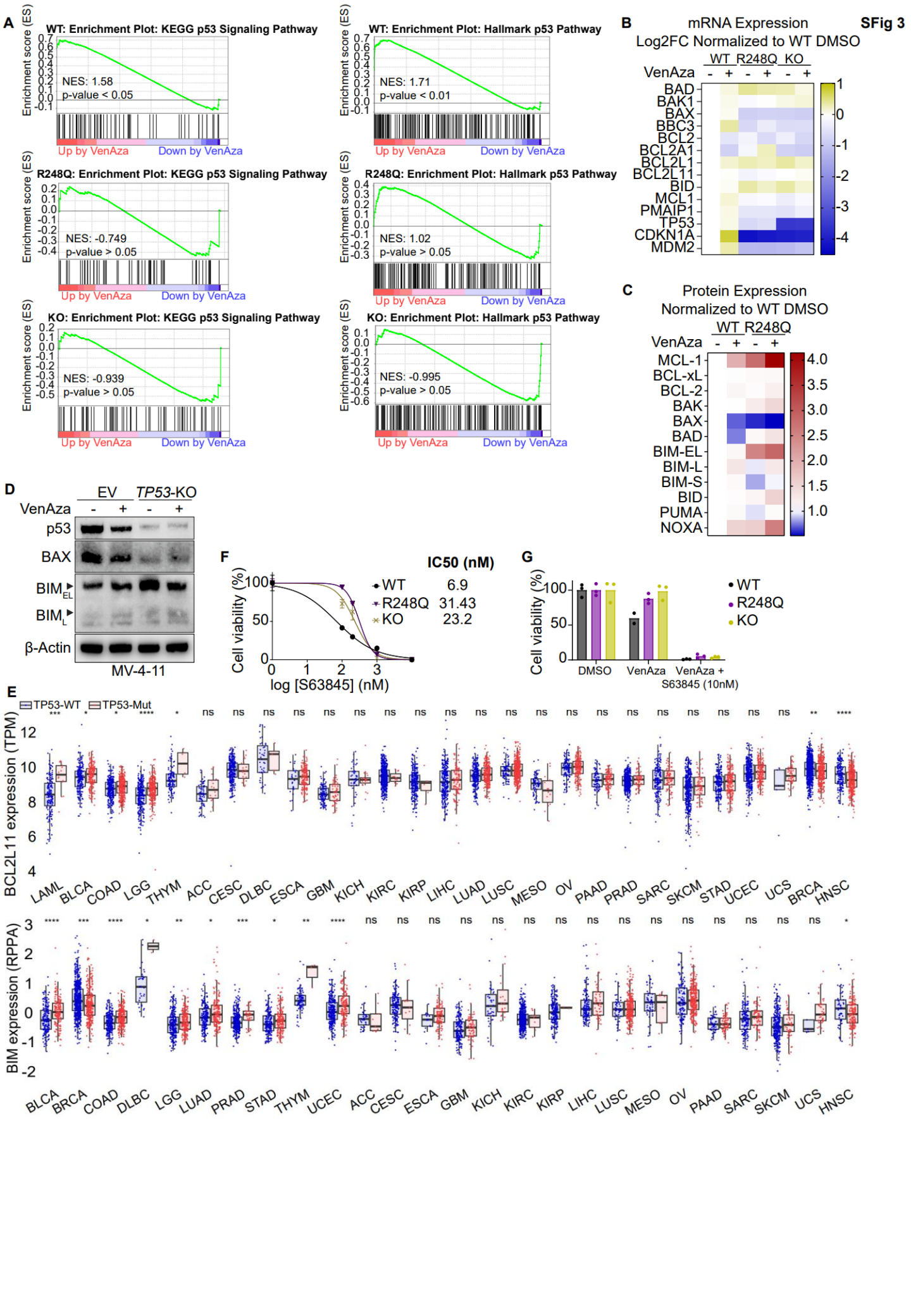
A
WT: Enrichment Plot: KEGG p53 Signaling Pathway
NES: 1.58
p-value < 0.05
WT: Enrichment Plot: Hallmark p53 Pathway
NES: 1.71
p-value < 0.01
R248Q: Enrichment Plot: KEGG p53 Signaling Pathway
NES: -0.749
p-value > 0.05
R248Q: Enrichment Plot: Hallmark p53 Pathway
NES: 1.02
p-value > 0.05
KO: Enrichment Plot: KEGG p53 Signaling Pathway
NES: -0.939
p-value > 0.05
KO: Enrichment Plot: Hallmark p53 Pathway
NES: -0.995
p-value > 0.05
Enrichment score (ES)
Up by VenAza
Down by VenAza
B
mRNA Expression
Log2FC Normalized to WT DMSO
WT R248Q KO
VenAza - + - + - +
BAD
BAK1
BAX
BBC3
BCL2
BCL2A1
BCL2L1
BCL2L11
BID
MCL1
PMAIP1
TP53
CDKN1A
MDM2
C
Protein Expression
Normalized to WT DMSO
WT R248Q
VenAza - + - +
MCL-1
BCL-xL
BCL-2
BAK
BAX
BAD
BIM-EL
BIM-L
BIM-S
BID
PUMA
NOXA
D
EV TP53-KO
VenAza - + - +
p53
BAX
BIM EL
BIM L
β-Actin
MV-4-11
F
IC50 (nM)
WT 6.9
R248Q 31.43
KO 23.2
Cell viability (%)
log [S63845] (nM)
G
Cell viability (%)
DMSO
VenAza
VenAza + S63845 (10nM)
WT
R248Q
KO
E
TP53-WT
TP53-Mut
BCL2L11 expression (TPM)
LAML BLCA COAD LGG THYM ACC CESC DLBC ESCA GBM KICH KIRC KIRP LIHC LUAD LUSC MESO OV PAAD PRAD SARC SKCM STAD UCEC UCS BRCA HNSC
BIM expression (RPPA)
BLCA BRCA COAD DLBC LGG LUAD PRAD STAD THYM UCEC ACC CESC ESCA GBM KICH KIRC KIRP LIHC LUSC MESO OV PAAD SARC SKCM UCS HNSC

SFig 4

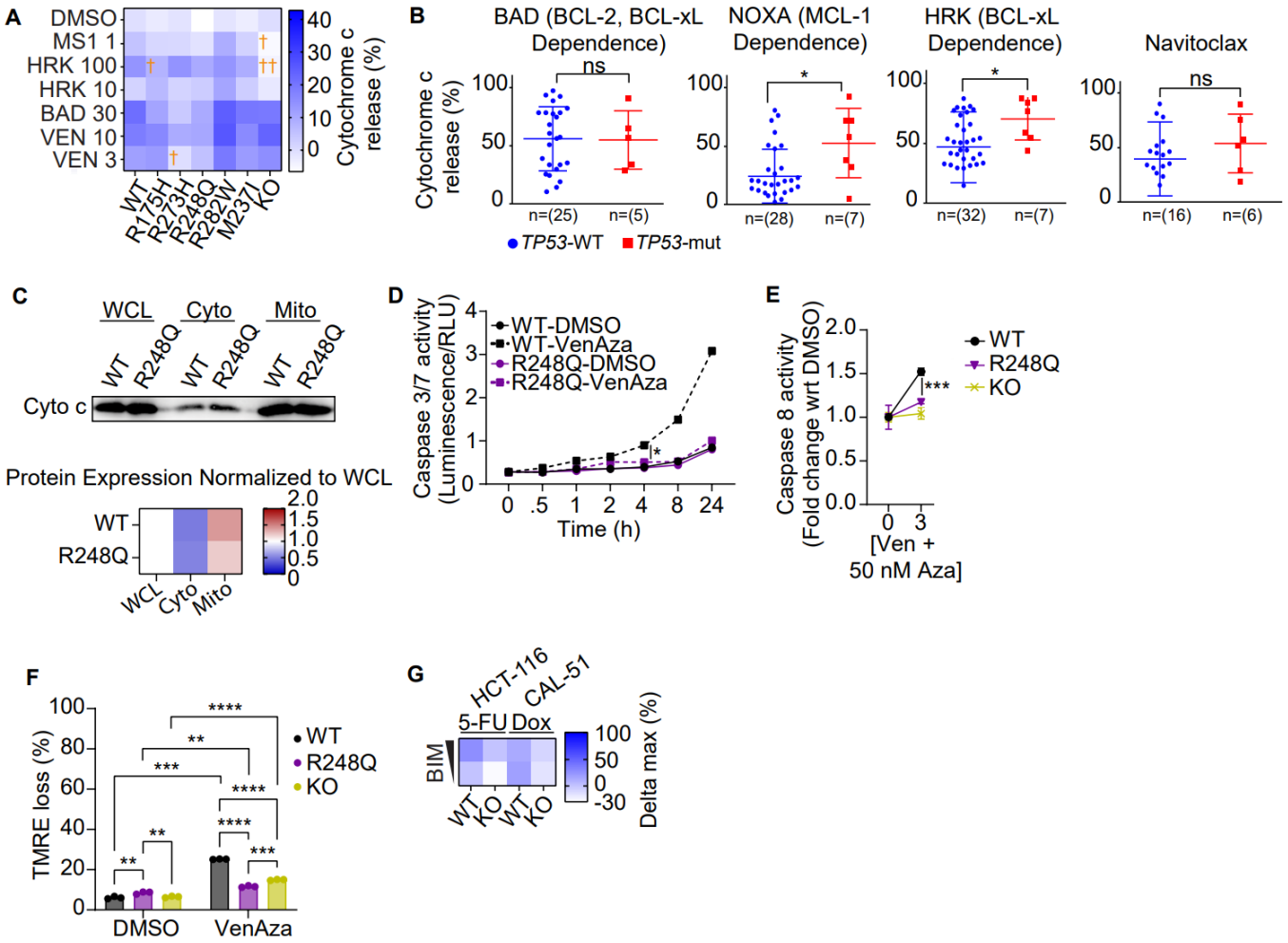
A
DMSO
MS1 1
HRK 100
HRK 10
BAD 30
VEN 10
VEN 3
WT
R175H
R273H
R248Q
R282W
M237I
KO
Cytochrome c release (%)
B
BAD (BCL-2, BCL-xL Dependence)
NOXA (MCL-1 Dependence)
HRK (BCL-xL Dependence)
Navitoclax
Cytochrome c release (%)
ns
n=(25)
n=(5)
n=(28)
n=(7)
n=(32)
n=(7)
n=(16)
n=(6)
TP53-WT
TP53-mut
C
WCL
Cyto
Mito
Cyto c
Protein Expression Normalized to WCL
D
WT-DMSO
WT-VenAza
R248Q-DMSO
R248Q-VenAza
Caspase 3/7 activity (Luminescence/RLU)
Time (h)
E
WT
R248Q
KO
Caspase 8 activity (Fold change wrt DMSO)
[Ven + 50 nM Aza]
F
TMRE loss (%)
DMSO
VenAza
G
HCT-116
CAL-51
5-FU
Dox
BIM
Delta max (%)

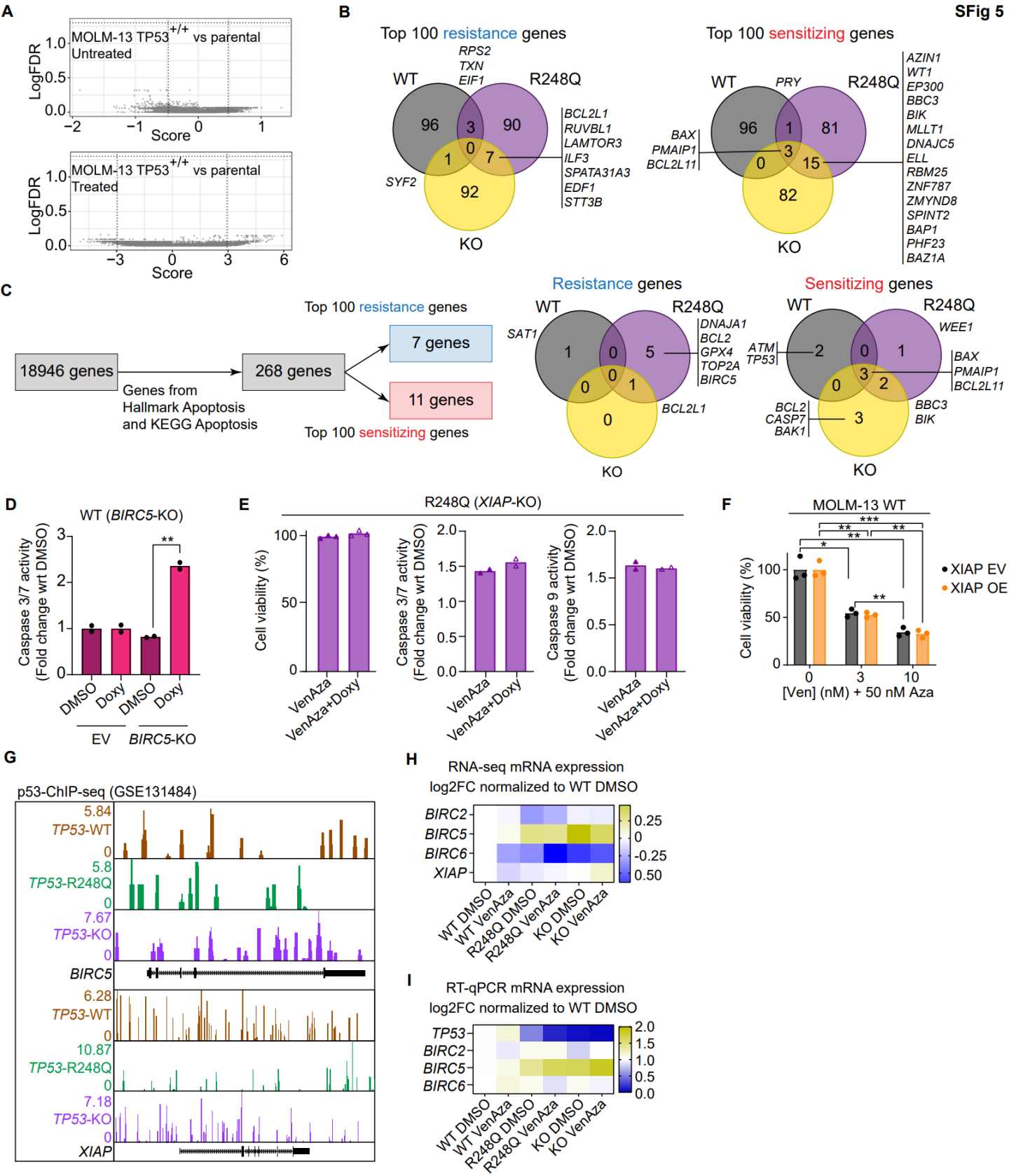
A
MOLM-13 TP53+/+ vs parental
Untreated
Treated
LogFDR
Score
B
Top 100 resistance genes
Top 100 sensitizing genes
WT
R248Q
KO
RPS2
TXN
EIF1
SYF2
BCL2L1
RUVBL1
LAMTOR3
ILF3
SPATA31A3
EDF1
STT3B
PRY
BAX
PMAIP1
BCL2L11
AZIN1
WT1
EP300
BBC3
BIK
MLLT1
DNAJC5
ELL
RBM25
ZNF787
ZMYND8
SPINT2
BAP1
PHF23
BAZ1A
C
18946 genes
Genes from Hallmark Apoptosis and KEGG Apoptosis
268 genes
Top 100 resistance genes
7 genes
11 genes
Top 100 sensitizing genes
Resistance genes
Sensitizing genes
SAT1
DNAJA1
BCL2
GPX4
TOP2A
BIRC5
BCL2L1
ATM
TP53
WEE1
BAX
PMAIP1
BCL2L11
BCL2
CASP7
BAK1
BBC3
BIK
D
WT (BIRC5-KO)
Caspase 3/7 activity (Fold change wrt DMSO)
DMSO
Doxy
EV
BIRC5-KO
E
R248Q (XIAP-KO)
Cell viability (%)
Caspase 3/7 activity (Fold change wrt DMSO)
Caspase 9 activity (Fold change wrt DMSO)
VenAza
VenAza+Doxy
F
MOLM-13 WT
Cell viability (%)
XIAP EV
XIAP OE
[Ven] (nM) + 50 nM Aza
G
p53-ChIP-seq (GSE131484)
TP53-WT
TP53-R248Q
TP53-KO
BIRC5
XIAP
H
RNA-seq mRNA expression
log2FC normalized to WT DMSO
BIRC2
BIRC5
BIRC6
XIAP
WT DMSO
WT VenAza
R248Q DMSO
R248Q VenAza
KO DMSO
KO VenAza
I
RT-qPCR mRNA expression
log2FC normalized to WT DMSO
TP53
BIRC2
BIRC5
BIRC6

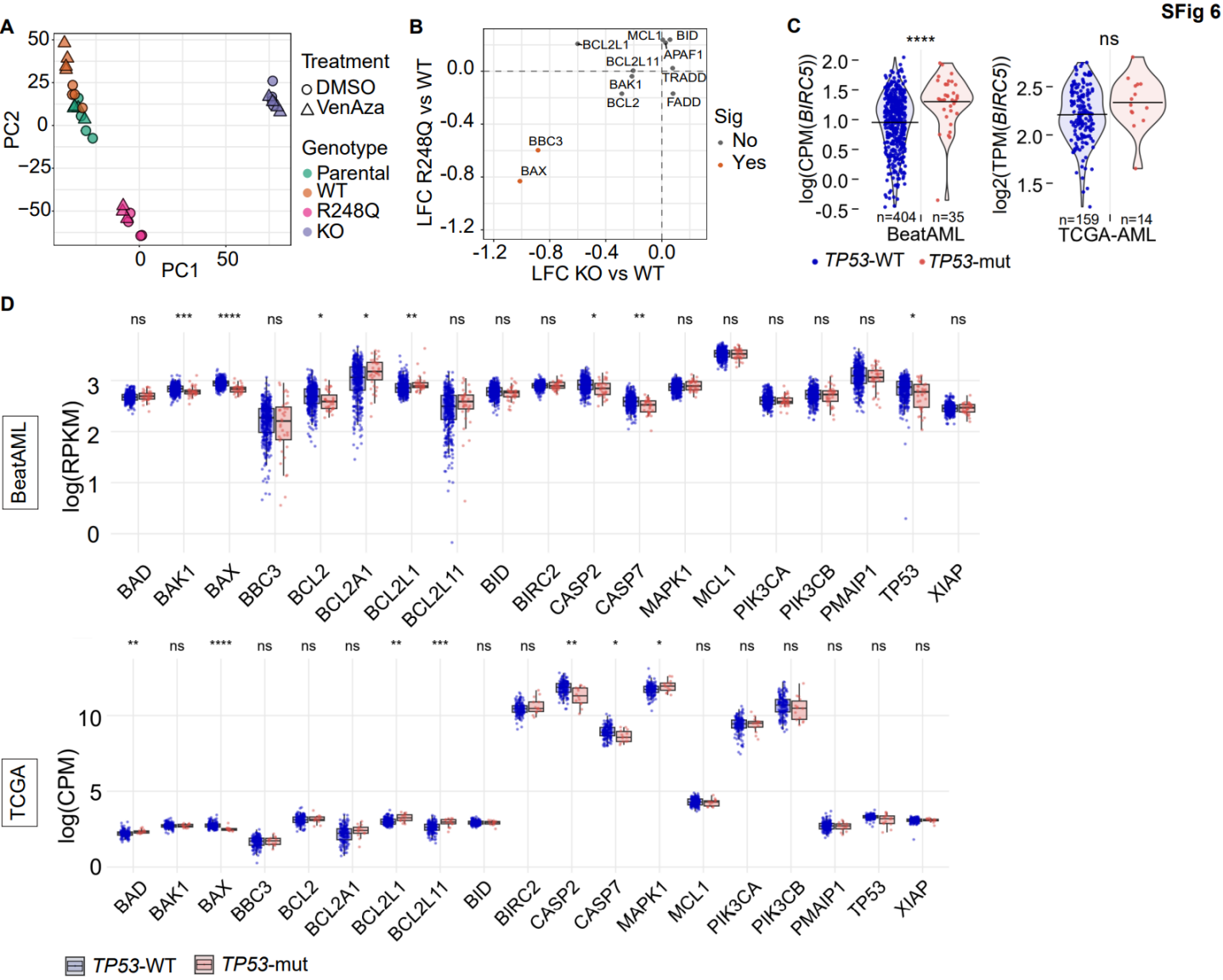
A
PC2
PC1
Treatment
DMSO
VenAza
Genotype
Parental
WT
R248Q
KO
B
LFC R248Q vs WT
LFC KO vs WT
BCL2L1
MCL1
BID
BCL2L11
APAF1
TRADD
BAK1
BCL2
FADD
BBC3
BAX
Sig
No
Yes
C
****
ns
log(CPM(BIRC5))
log2(TPM(BIRC5))
n=404
n=35
BeatAML
n=159
n=14
TCGA-AML
TP53-WT
TP53-mut
D
BeatAML
log(RPKM)
BAD
BAK1
BAX
BBC3
BCL2
BCL2A1
BCL2L1
BCL2L11
BID
BIRC2
CASP2
CASP7
MAPK1
MCL1
PIK3CA
PIK3CB
PMAIP1
TP53
XIAP
TCGA
log(CPM)
TP53-WT
TP53-mut

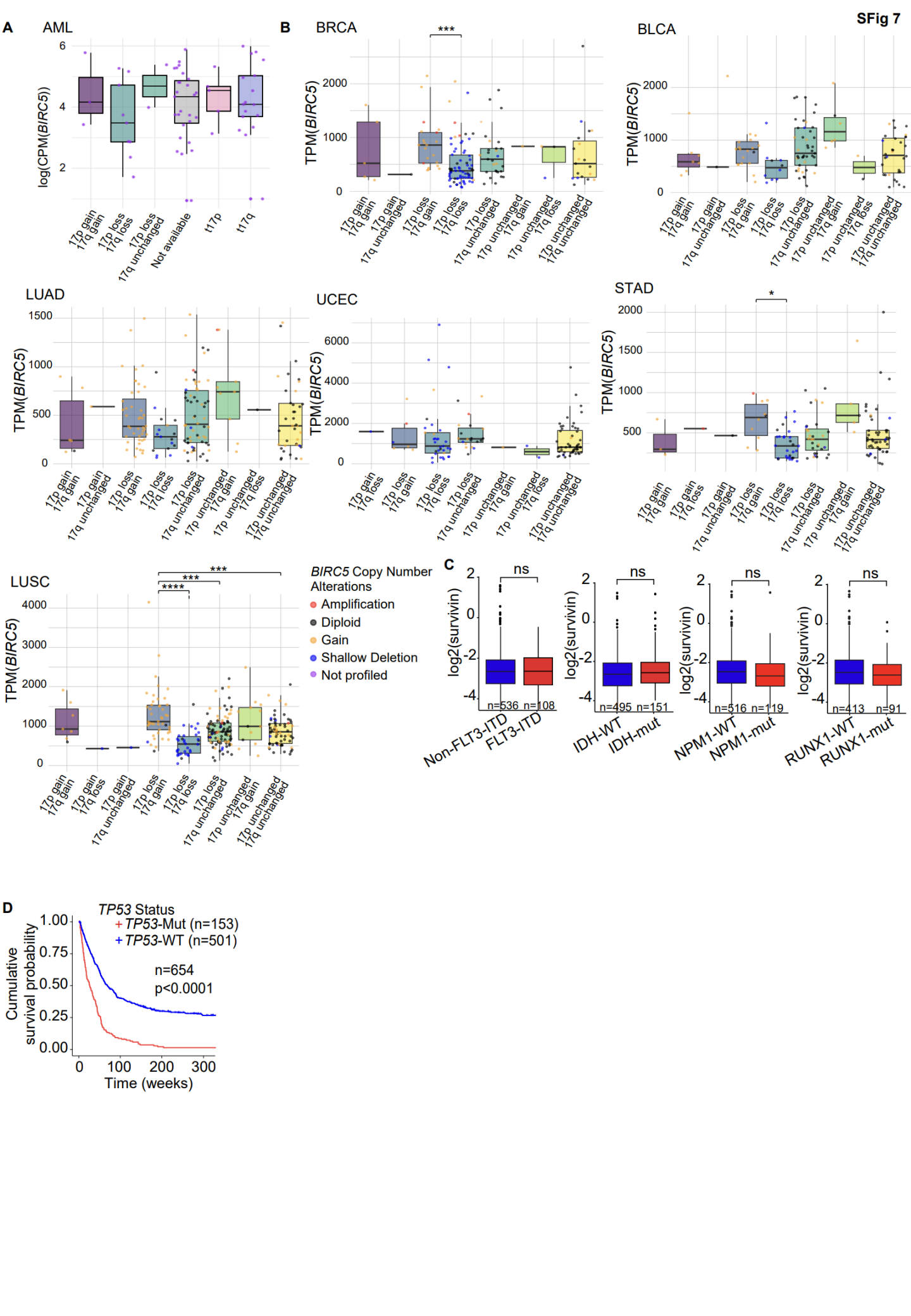
SFig 7
A
AML
log(CPM(BIRC5))
17p gain 17q gain
17p loss 17q loss
17p loss 17q unchanged
Not available
t17p
t17q
B
BRCA
BLCA
LUAD
UCEC
STAD
LUSC
TPM(BIRC5)
BIRC5 Copy Number Alterations
Amplification
Diploid
Gain
Shallow Deletion
Not profiled
C
log2(survivin)
ns
n=536 n=108
Non-FLT3-ITD
FLT3-ITD
n=495 n=151
IDH-WT
IDH-mut
n=516 n=119
NPM1-WT
NPM1-mut
n=413 n=91
RUNX1-WT
RUNX1-mut
D
TP53 Status
TP53-Mut (n=153)
TP53-WT (n=501)
n=654
p<0.0001
Cumulative survival probability
Time (weeks)

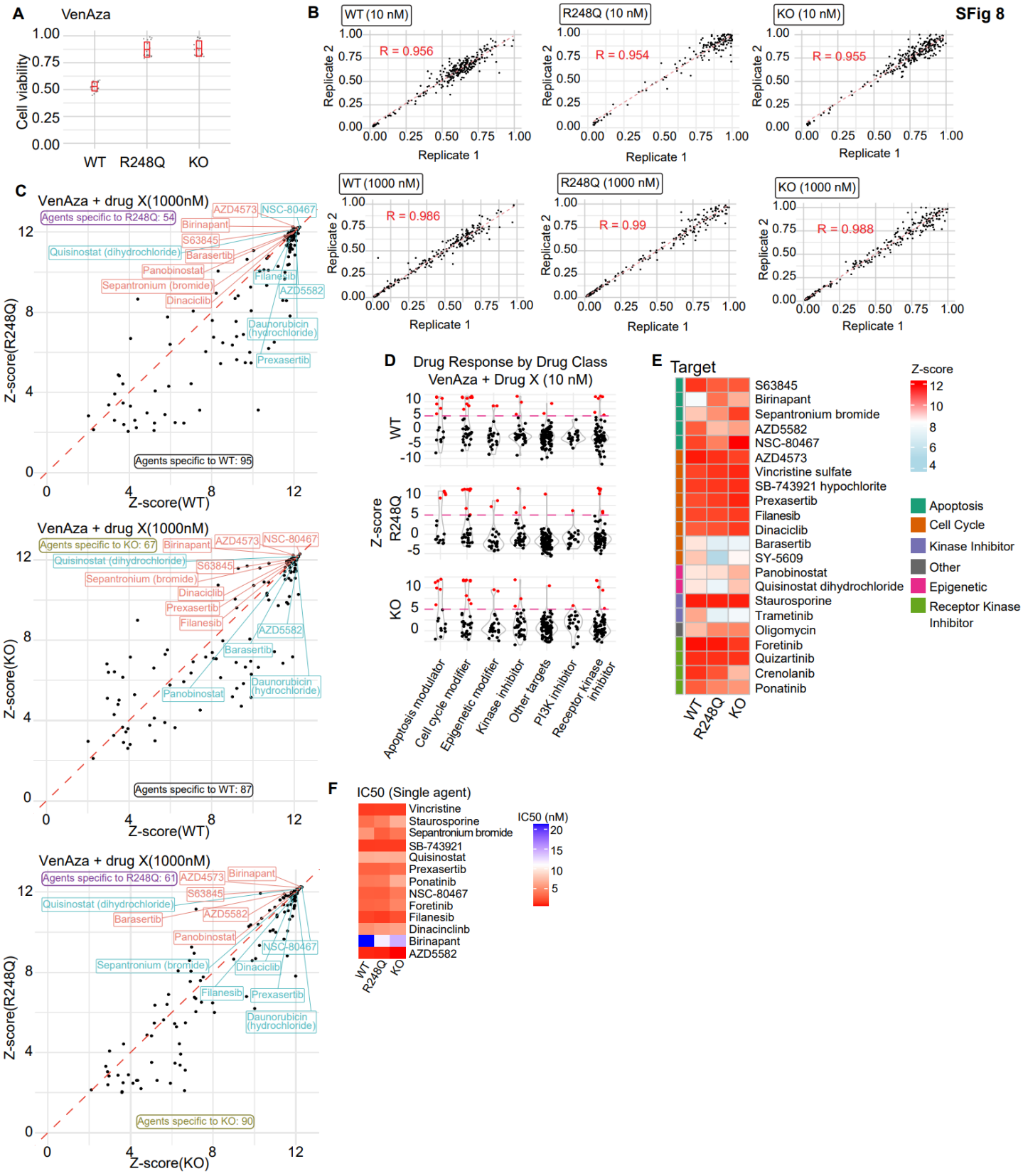
SFig 8
A
VenAza
Cell viability
WT
R248Q
KO
B
WT (10 nM)
R248Q (10 nM)
KO (10 nM)
R = 0.956
R = 0.954
R = 0.955
WT (1000 nM)
R248Q (1000 nM)
KO (1000 nM)
R = 0.986
R = 0.99
R = 0.988
Replicate 1
Replicate 2
C
VenAza + drug X(1000nM)
Agents specific to R248Q: 54
Agents specific to WT: 95
Agents specific to KO: 67
Agents specific to WT: 87
Agents specific to R248Q: 61
Agents specific to KO: 90
Z-score(WT)
Z-score(KO)
Z-score(R248Q)
AZD4573
NSC-80467
Birinapant
S63845
Quisinostat (dihydrochloride)
Barasertib
Panobinostat
Sepantronium (bromide)
Dinaciclib
Filanesib
AZD5582
Daunorubicin (hydrochloride)
Prexasertib
D
Drug Response by Drug Class
VenAza + Drug X (10 nM)
Z-score
WT
R248Q
KO
Apoptosis modulator
Cell cycle modifier
Epigenetic modifier
Kinase inhibitor
Other targets
PI3K inhibitor
Receptor kinase inhibitor
E
Target
Z-score
S63845
Birinapant
Sepantronium bromide
AZD5582
NSC-80467
AZD4573
Vincristine sulfate
SB-743921 hypochlorite
Prexasertib
Filanesib
Dinaciclib
Barasertib
SY-5609
Panobinostat
Quisinostat dihydrochloride
Staurosporine
Trametinib
Oligomycin
Foretinib
Quizartinib
Crenolanib
Ponatinib
Apoptosis
Cell Cycle
Kinase Inhibitor
Other
Epigenetic
Receptor Kinase Inhibitor
F
IC50 (Single agent)
IC50 (nM)
Vincristine
Staurosporine
Sepantronium bromide
SB-743921
Quisinostat
Prexasertib
Ponatinib
NSC-80467
Foretinib
Filanesib
Dinacinclinb
Birinapant
AZD5582

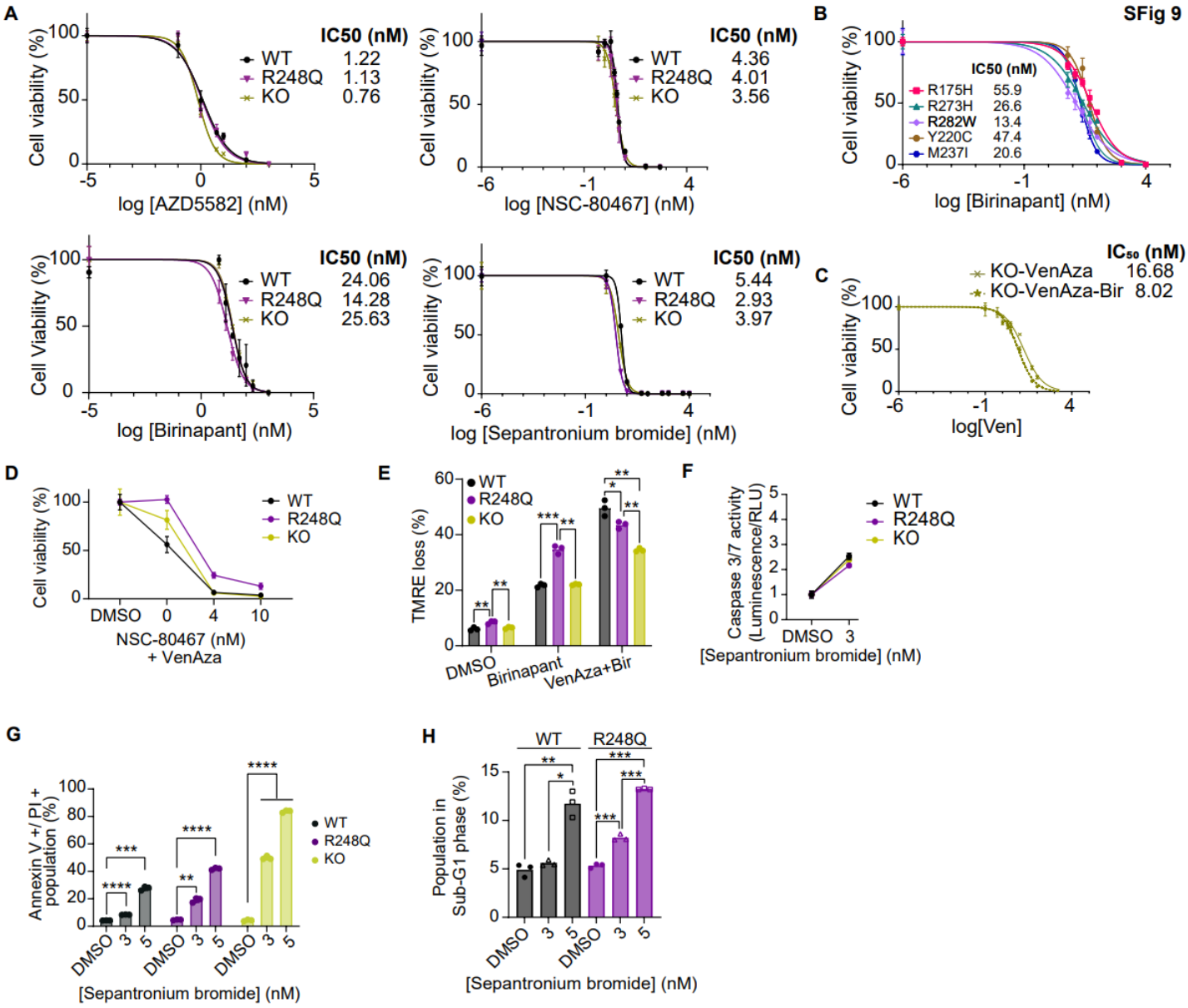
SFig 9
A
Cell viability (%)
log [AZD5582] (nM)
IC50 (nM)
WT 1.22
R248Q 1.13
KO 0.76
log [NSC-80467] (nM)
WT 4.36
R248Q 4.01
KO 3.56
B
log [Birinapant] (nM)
IC50 (nM)
R175H 55.9
R273H 26.6
R282W 13.4
Y220C 47.4
M237I 20.6
Cell Viability (%)
WT 24.06
R248Q 14.28
KO 25.63
log [Sepantronium bromide] (nM)
WT 5.44
R248Q 2.93
KO 3.97
C
IC50 (nM)
KO-VenAza 16.68
KO-VenAza-Bir 8.02
log[Ven]
D
NSC-80467 (nM)
+ VenAza
DMSO
E
TMRE loss (%)
Birinapant
VenAza+Bir
F
Caspase 3/7 activity (Luminescence/RLU)
[Sepantronium bromide] (nM)
G
Annexin V +/ PI + population (%)
H
WT
R248Q
Population in Sub-G1 phase (%)

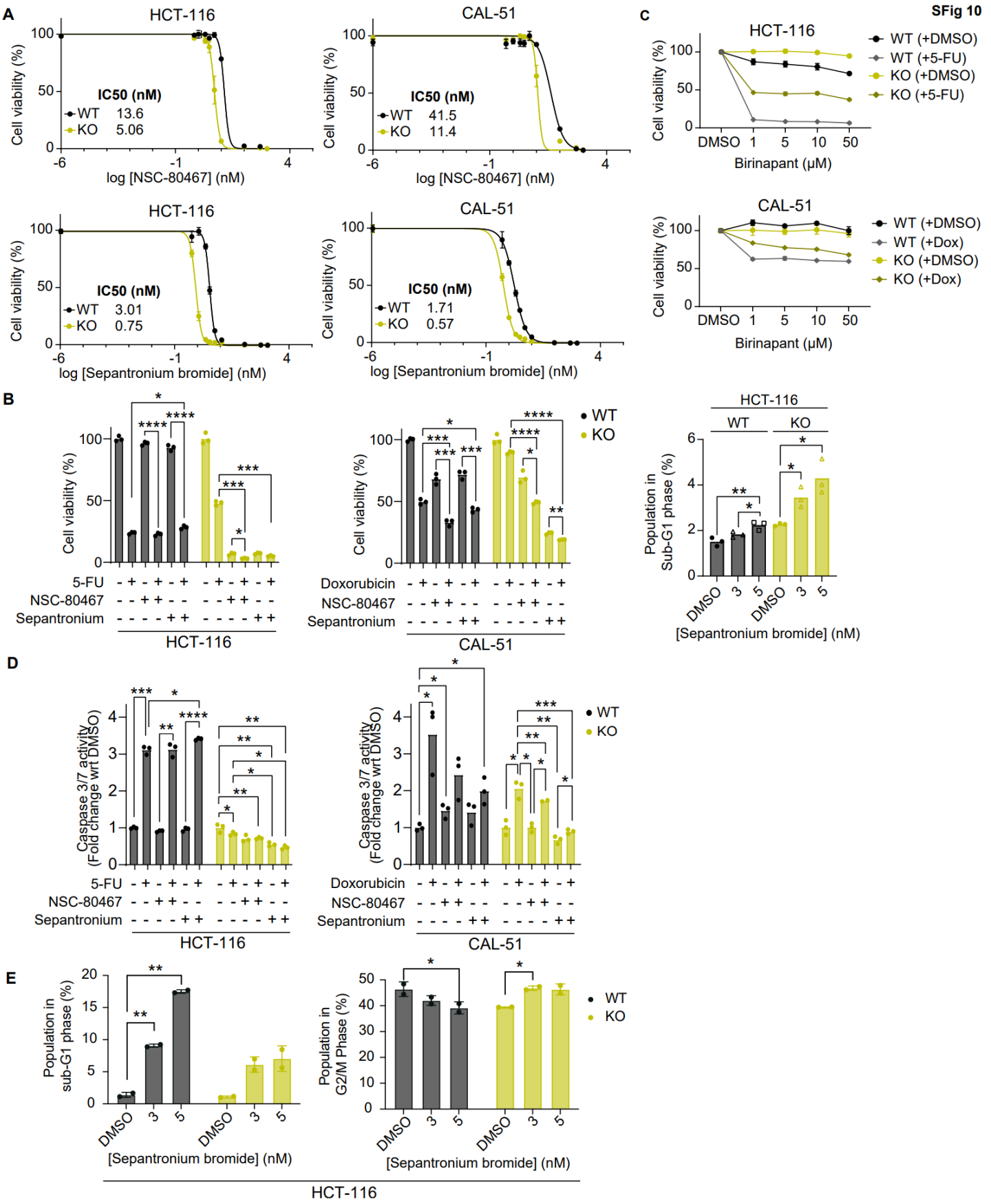
SFig 10
A
HCT-116
CAL-51
Cell viability (%)
IC50 (nM)
WT 13.6
KO 5.06
WT 41.5
KO 11.4
log [NSC-80467] (nM)
WT 3.01
KO 0.75
WT 1.71
KO 0.57
log [Sepantronium bromide] (nM)
C
WT (+DMSO)
WT (+5-FU)
KO (+DMSO)
KO (+5-FU)
WT (+Dox)
KO (+Dox)
Birinapant (μM)
B
5-FU
NSC-80467
Sepantronium
Doxorubicin
WT
KO
Population in Sub-G1 phase (%)
[Sepantronium bromide] (nM)
D
Caspase 3/7 activity (Fold change wrt DMSO)
E
Population in sub-G1 phase (%)
Population in G2/M Phase (%)

SFig 11

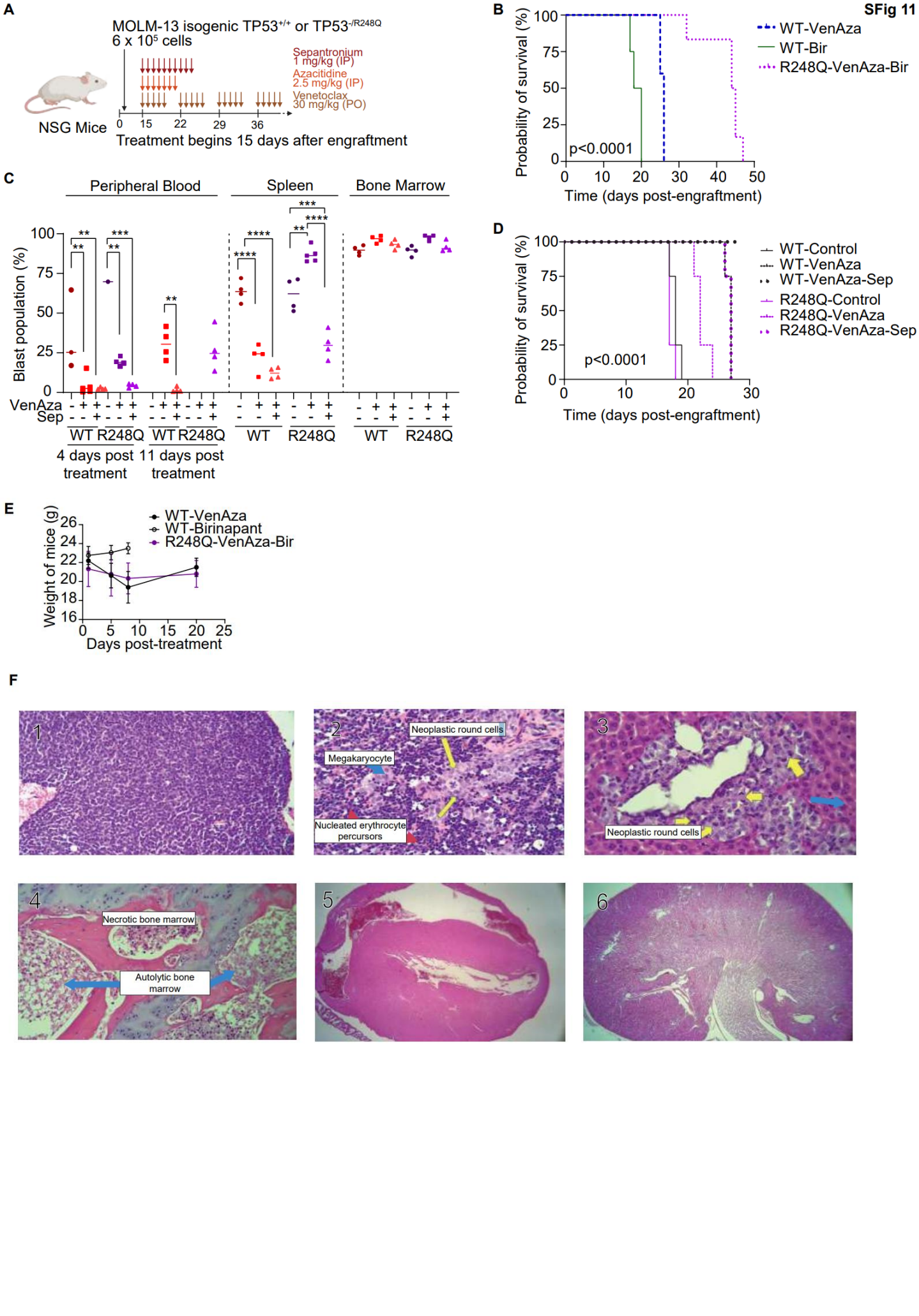
A
MOLM-13 isogenic TP53+/+ or TP53-/R248Q
6 x 10^5 cells
Sepantronium 1 mg/kg (IP)
Azacitidine 2.5 mg/kg (IP)
Venetoclax 30 mg/kg (PO)
NSG Mice
0 15 22 29 36
Treatment begins 15 days after engraftment
B
Probability of survival (%)
Time (days post-engraftment)
p<0.0001
WT-VenAza
WT-Bir
R248Q-VenAza-Bir
C
Peripheral Blood
Spleen
Bone Marrow
Blast population (%)
VenAza
Sep
WT R248Q WT R248Q
4 days post treatment
11 days post treatment
WT R248Q
WT R248Q
D
Probability of survival (%)
Time (days post-engraftment)
p<0.0001
WT-Control
WT-VenAza
WT-VenAza-Sep
R248Q-Control
R248Q-VenAza
R248Q-VenAza-Sep
E
Weight of mice (g)
Days post-treatment
WT-VenAza
WT-Birinapant
R248Q-VenAza-Bir
F
1
2
Neoplastic round cells
Megakaryocyte
Nucleated erythrocyte percursors
3
Neoplastic round cells
4
Necrotic bone marrow
Autolytic bone marrow
5
6

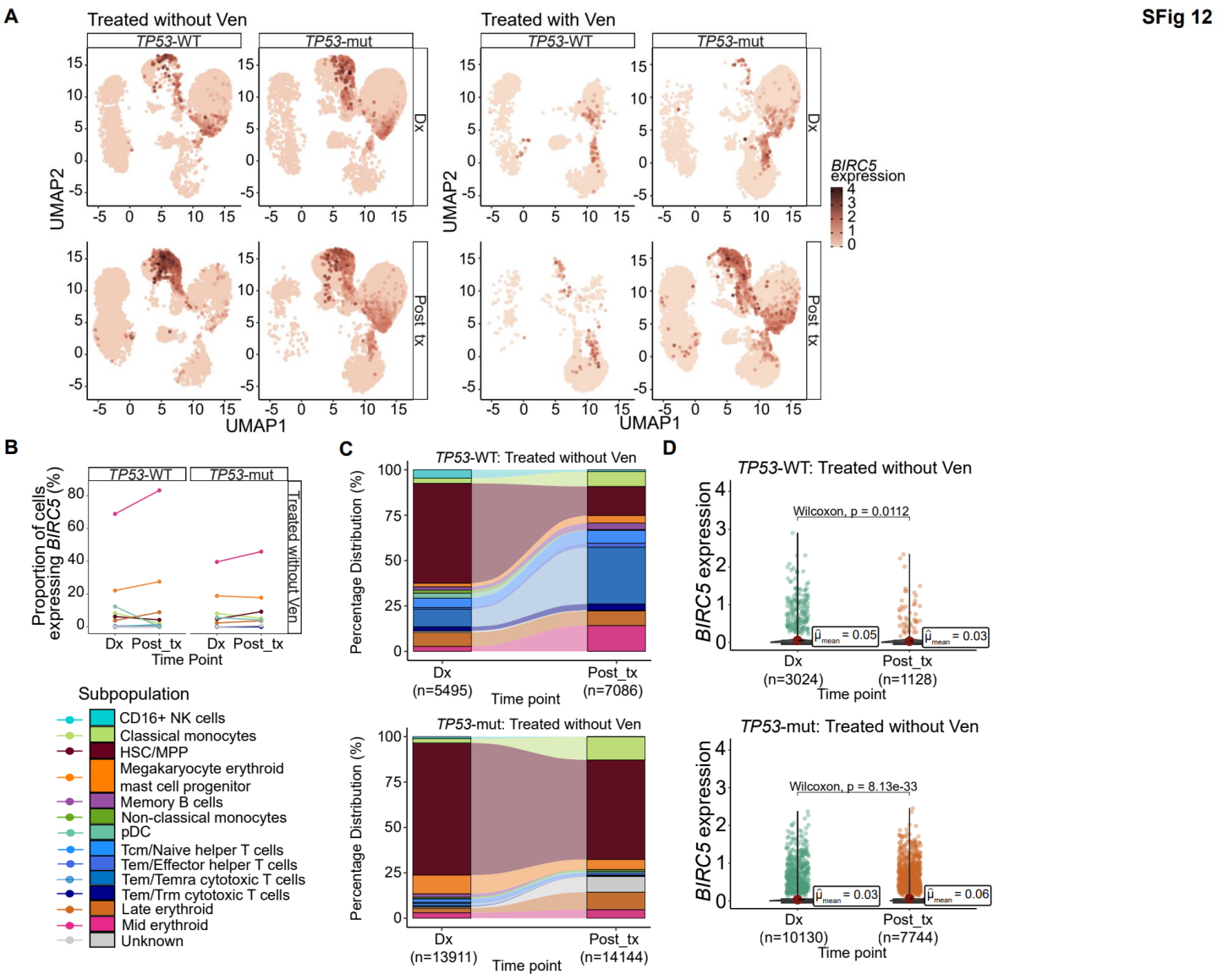
A
Treated without Ven
Treated with Ven
TP53-WT
TP53-mut
Dx
Post_tx
UMAP2
UMAP1
BIRC5 expression
B
Proportion of cells expressing BIRC5 (%)
Treated without Ven
Time Point
Subpopulation
CD16+ NK cells
Classical monocytes
HSC/MPP
Megakaryocyte erythroid mast cell progenitor
Memory B cells
Non-classical monocytes
pDC
Tcm/Naive helper T cells
Tem/Effector helper T cells
Tem/Temra cytotoxic T cells
Tem/Trm cytotoxic T cells
Late erythroid
Mid erythroid
Unknown
C
TP53-WT: Treated without Ven
Percentage Distribution (%)
Dx (n=5495)
Post_tx (n=7086)
Time point
TP53-mut: Treated without Ven
Dx (n=13911)
Post_tx (n=14144)
D
TP53-WT: Treated without Ven
BIRC5 expression
Wilcoxon, p = 0.0112
μ̂mean = 0.05
μ̂mean = 0.03
Dx (n=3024)
Post_tx (n=1128)
Time point
TP53-mut: Treated without Ven
Wilcoxon, p = 8.13e-33
μ̂mean = 0.03
μ̂mean = 0.06
Dx (n=10130)
Post_tx (n=7744)